Early-type objects in NGC6611 and the Eagle Nebula.

Christophe Martayan, Michele Floquet, Anne-Marie Hubert, Coralie Neiner, Yves Fremat, Dietrich Baade, Juan Fabregat

Astronomy & Astrophysics manuscript no. article5e03.hyper22573
June 9, 2008

Early-type objects in NGC 6611 and Eagle Nebula.

C. Martayan[1,2], M. Floquet[2], A.M. Hubert[2], C. Neiner[2], Y. Frémat[1], D. Baade[3], and J. Fabregat[4]

[1] Royal Observatory of Belgium, 3 avenue circulaire, 1180 Brussels, Belgium
[2] GEPI, Observatoire de Paris, CNRS, Université Paris Diderot; 5 place Jules Janssen 92195 Meudon Cedex, France
[3] European Organisation for Astronomical Research in the Southern Hemisphere, Karl-Schwarzschild-Str. 2, D-85748 Garching b. Muenchen, Germany
[4] Observatorio Astronómico de Valencia, edifici Instituts d'investigació, Poligon la Coma, 46980 Paterna Valencia, Spain

Received /Accepted

ABSTRACT

Aims. An important question about Be stars is whether Be stars are born as Be stars or whether they become Be stars during their evolution. It is necessary to observe young clusters to answer this question.
Methods. To this end, observations of stars in NGC 6611 and the star-formation region of Eagle Nebula have been carried out with the ESO-WFI in slitless spectroscopic mode and at the VLT-GIRAFFE (R$\simeq$ 6400–17000). The targets for the GIRAFFE observations were pre-selected from the literature and our catalogue of emission-line stars based on the WFI study. GIRAFFE observations allowed us to study accurately the population of the early-type stars with and without emission lines. For this study, we determined the fundamental parameters of OBA stars thanks to the GIRFIT code. We also studied the status of the objects (main sequence or pre-main sequence stars) by using IR data, membership probabilities, and location in HR diagrams.
Results. The nature of the early-type stars with emission-line stars in NGC 6611 and its surrounding environment is derived. The slitless observations with the WFI clearly indicate a small number of emission-line stars in M16. We observed with GIRAFFE 101 OBA stars, among them 9 are emission-line stars with circumstellar emission in Hα. We found that: W080 could be a new He-strong star, like W601. W301 is a possible classical Be star, W503 is a mass-transfer eclipsing binary with an accretion disk, and the other ones are possible Herbig Ae/Be stars. We also found that the rotational velocities of main sequence B stars are 18% lower than those of pre-main sequence B stars, in good agreement with theory about the evolution of rotational velocities. Combining adaptive optics, IR data, spectroscopy, and radial velocity indications, we found that 27% of the B-type stars are binaries. We also redetermined the age of NGC 6611 found equal to 1.2–1.8 Myears in good agreement with the most recent determinations.

Key words. Stars: early-type – Stars: emission-line, Be – Stars: fundamental parameters – Stars: evolution – Stars: pre-main sequence

1. Introduction

The origin of the Be phenomenon, i.e. periods of spectral emission due to the presence of a circumstellar envelope around Be stars, is still debated. Rapid rotation seems to be a major key in triggering this phenomenon. To understand the Be phenomenon, it is important to know at which phase of the stellar evolution on the main sequence (MS) it appears.

According to a statistical study of Be stars in clusters, Fabregat & Torrejón (2000) concluded that it may occur in the second half of the MS phase. Taking into account effects due to fast rotation, Zorec et al. (2005) estimated that the appearance of the Be phenomenon among field early-type stars is probably mass-dependent and that it may appear at any time during the MS phase. Martayan et al. (2006a, 2007) showed that the appearance of Be stars is mass-, and metallicity-dependent. In the field of Milky Way (MW), they found that less massive Be stars only appear during the second part of the MS, while massive Be stars appear mainly during the first part of the MS, and the intermediate-mass Be stars appear during the whole MS.

To confirm this, it is necessary to observe young or very young open clusters with emission-line stars (ELS).

NGC 6611 in M16 is a very young cluster previously known to contain a large number of ELS (Hillenbrand et al. 1993; de Winter et al. 1997), which have been included in the reference database SIMBAD and WEBDA. However, the investigation of the ELS character was made

Send offprint requests to: C. Martayan
Correspondence to: Martayan@oma.be

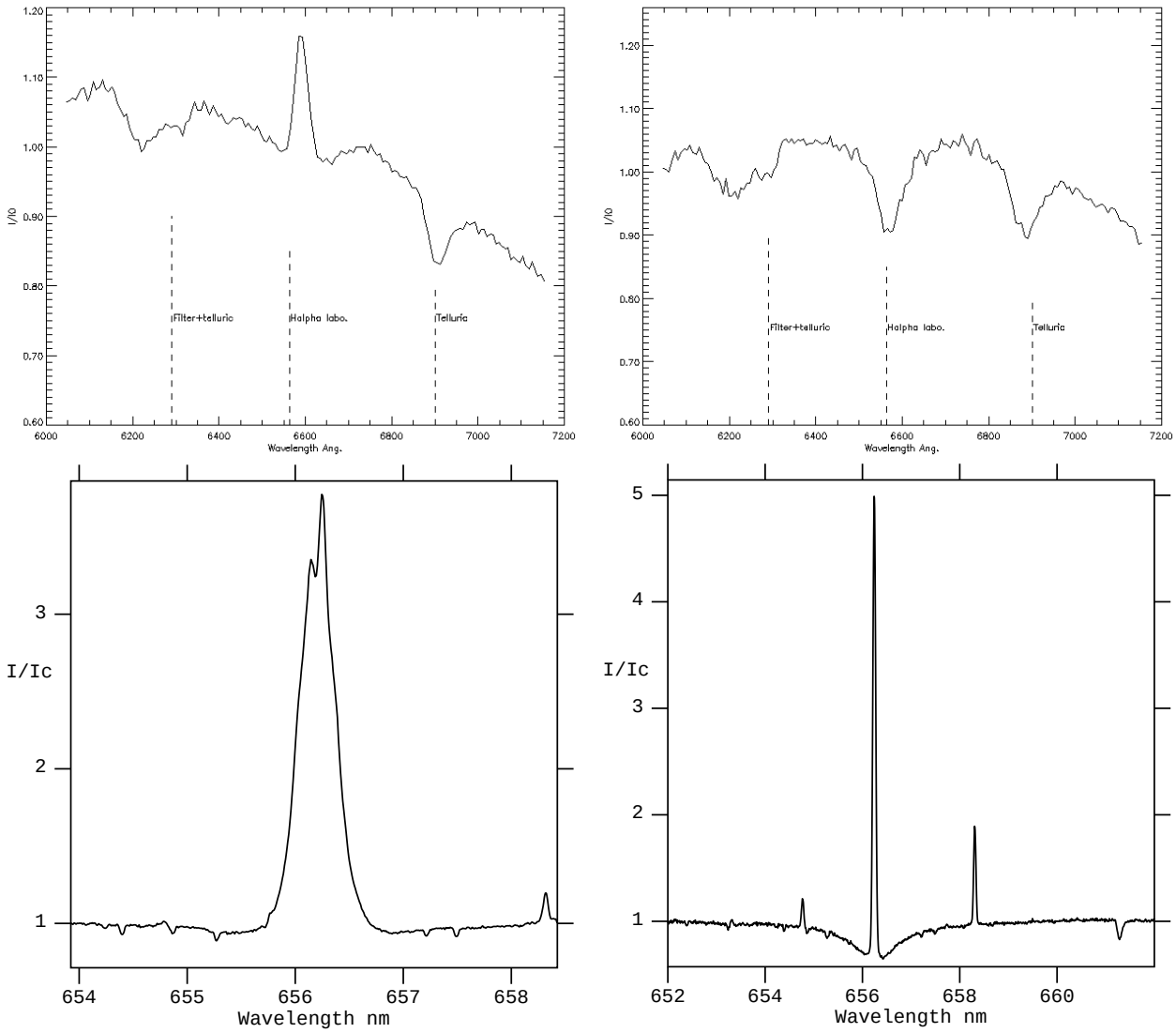

Fig. 2. Left: Hα spectra of the true ELS star W483. Top-left: spectrum, scaled to the mean value of its continuum, obtained with the WFI in slitless spectroscopic mode. Bottom-left: spectrum, normalized to its continuum, obtained with the VLT-GIRAFFE. In this last spectrum, the circumstellar and nebular Hα emissions are visible. Right: Hα spectra of the star W371. Top-right: spectrum, scaled to the mean value of its continuum, obtained with the WFI in slitless spectroscopic mode. Bottom-right: spectrum with nebular emission line, normalized to its continuum, obtained with the VLT-GIRAFFE. Only nebular emission is present.

from low and moderate resolution spectra, which did not allow to distinguish intrinsic stellar emission from nebular emission as noted by Hillenbrand et al. (1993). Using deep objective prism spectroscopy, which is not sensitive to nebular lines, Herbig & Dahm (2001) only identified a small number of ELS at the opposite of the other studies. This was recently confirmed by Evans et al. (2005) who observed the more massive population of NGC 6611 with high-resolution spectroscopy (FLAMES and FEROS at ESO). With the ESO-WFI in slitless spectroscopic mode and the VLT-GIRAFFE, we performed observations from late O to early A type stars in NGC 6611 and surrounding fields, which are thought to be still in formation stages (see e.g. Indebetouw et al. 2007), in order to analyse the B star population with and without emission lines. In the present paper we report on the detection of new ELS in the NGC 6611 region, we determined the fundamental parameters and studied: (i) the evolution of rotational velocities between pre-main sequence phase and main sequence, (ii) the age-distributions of objects in M16, (iii) the evolutionary status of each B-type star, as well as the nature of the emission/absorption stars: pre-main sequence stars or HAeBe (ELS), or main-sequence stars or classical Be stars (ELS).

2. Observations/Reduction

NGC 6611 lies in the star-formation region of the complex Eagle nebula. The ESO-WFI in its slitless spectroscopic mode and the high-resolution VLT-FLAMES spec-

troscopy allow us to check, on the case by case basis, if there is emission and if it is of nebular or circumstellar origin.

2.1. ESO-WFI in spectroscopic mode

The Wide Field Imager (WFI) is attached to the 2.2m MPG telescope at La Silla. Observations[1] with WFI were obtained on September 26, 2002. The WFI has a field of view of $33' \times 34'$. We used the R50 grism and the Rc162 filter centered on Hα with a bandpass of 200 nm and a resolution lower than 1000 (see Baade et al. 1999). The two images were obtained with respectively 120 and 450s exposure times, which allow to detect the continuum of faint sources (V$\sim$19). However, we only need brightest stars (up to V$\sim$15), which represent the OB-type population in the formation region; their spectra have sufficient signal to noise ratio to detect reliably Hα emission. Note that the first image (120s exposed) is used to study the brightest stars, which are saturated in the second more exposed image of our data.

This special slitless mode is sensitive neither to the nebular lines nor to the weak circumstellar emission. However, it is easy to detect ELS with sufficient circumstellar emission in Hα. The image of the field of NGC 6611 (α(2000) = 18h18min42s, δ(2000) = -13°46′57.6″) in slitless spectroscopic mode is shown in Fig. .1.

The image reduction was performed with IRAF[2] tasks and the MSCRED package. The extraction of spectra was performed using the SExtractor code (Bertin & Arnouts 1996) with special adapted convolution masks (provided by E. Bertin). About 15000 spectra have been extracted. Spectra of certain stars in the field are not available because they fall in the interCCDs spaces. Also note that certain spectra are contaminated by cosmic rays, by superimposed zeroth orders of other spectra or/and by other spectra.

The analysis of extracted spectra was performed individually with our IDL-based code (lecspec4). Examples of slitless spectra for one ELS with a circumstellar emission line at Hα (W483) and for one non-ELS (W371) are shown in Fig. 2 left and right respectively. A rough wavelength calibration, based on the theoretical dispersion law of the grism and Rc filter, is provided for the spectra (see Fig. 2. Astrometric calibration was performed with the ASTROM package (Wallace & Gray 2003) and refined with the UCAC2 catalogue.

We explored the NGC 6611 field towards the 19th V magnitude; several faint stars, like [OSP2002] BRC 30 4 from Ogura et al. (2002) (who used the same instrumentation than Herbig & Dahm (2001)), exhibit Hα emission. These targets are not B-type objects, but TTauri stars as explained by Ogura et al. (2002) and Herbig & Dahm (2001). However, we concentrate our study only on the stars with V magnitude up to 15 for our purpose.

A short list of 7 Hα ELS was finally obtained with WFI and are indicated in Table 1; 6 of them are in common with those recently confirmed/discovered by Herbig & Dahm (2001) and Evans et al. (2005), 1 ELS is a new detection. Note that ELS with weak emission (like W601 or W205) cannot be detected with such an instrumentation.

Similar observations were obtained for the open cluster Westerlund 1 in a field centered on (α(2000) = 16h46min47.9s, δ(2000) = -45°48′59″). The exposure times for the 2 images are 120 and 900s. We found several ELS previously known as Wolf-Rayet or Be stars. However, the spectra extracted are difficult to exploit due to the very faint luminosity of the stars. We mention here the existence of these observations to whom it may interest.

2.2. VLT-GIRAFFE

This work also makes use of spectra obtained with the multifibre spectrograph VLT-FLAMES (Pasquini et al. 2002) in Medusa mode (131 fibres) at medium and high resolutions. Observations with GIRAFFE[3] were carried out on April 14-15, 2004 in the young cluster NGC 6611 and in its surrounding field, as part of the Guaranteed Time Observation programmes of the Paris Observatory (P.I.: F. Hammer). The observed field (25′ in diameter) is centered at α(2000) = 18h18min50s and δ(2000) = $-13°49'30''$.

The HR15N setup (647–679 nm, R=17000) was used to identify Hα ELS, to study the Hα characteristics, and to determine the interstellar reddening of each target. The LR3 (450.1–507.8 nm, R=7500) setup was used for the Hβ line characteristics and the LR2 (396.4–456.7 nm, R=6400) setup for the determination of fundamental parameters. Two consecutive spectra were obtained in each setup and summed up. The exposure time was 2×1800s, 2×1000s, and 2×900s in the HR15N, LR3, LR2 setups, respectively.

The VLT-GIRAFFE targets were pre-selected from our WFI catalogue of ELS and from Hillenbrand et al. (1993), de Winter et al. (1997), and Herbig & Dahm (2001). OBA stars without emission were also pre-selected from CDS/SIMBAD. The location of observed stars with the VLT-GIRAFFE are shown in Fig. .3.

Bias, flat-fields and wavelength calibration (ThAr) exposures were obtained for each stellar exposure and used to reduce the spectra. The data reduction was performed with the dedicated software GIRBLDRS developed at the Geneva Observatory (see http://girbldrs.sourceforge.net) and with several tasks of the IRAF package for extraction, calibration and sky correction of the spectra. The heliocentric correction (-28 km s^{-1}) at the epoch of observations was applied to each stellar spectrum.

[1] ESO run 69.D-0275A

[2] IRAF is distributed by the National Optical Astronomy Observatories, which is operated by the Association of Universities for Research in Astronomy (AURA), Inc., under cooperative agreement with the National Science Foundation.

[3] ESO run 73.D-0133A

Table 1. Comparison of candidate ELS or Be stars found in NGC 6611 by different authors and in function of the technique used. Hillenbrand et al. (1993,and references therein), de Winter et al. (1997), Evans et al. (2005) used slit and/or fibre spectroscopy, Herbig & Dahm (2001) used slitless spectroscopy, and in our study we use slitless and fibre spectroscopy (WFI/GIRAFFE). "Abs" is for absorption line in Hα, "Em" is for emission line in Hα, "x" for no spectrum (WFI or GIRAFFE) or for no exploitable spectrum (WFI).

Stars	H93	W97	H01	E05	M07	Stars	H93	W97	H01	E05	M07	Stars	H93	W97	H01	E05	M07
WFI[N6611]017					Em/Em	W266		Em	cont		x/x	W374		Em	Abs		Abs/x
W031					x/Em	W267		Em	Abs	Abs	x/Abs	W388		Em	Abs		Abs/Abs
W080					x/Em	W273		Em	Abs		x/Abs	W389	Em		Abs		Abs/Abs
W112	Em		Abs		x/x	W280	Em			Abs	x/x	W396		Em	Abs		Abs/x
W138	Em		Abs		Abs/x	W281	Em		Abs		Abs/Abs	W400		Em	Abs	Abs	Abs/Abs
W181	Em				Abs/x	W297	abs	Em	Abs	Abs	Abs/x	W455		Em	Abs	Abs	Abs/Abs
W198	Em				Abs/x	W299	Em	Em	Abs		x/Abs	W469	Em	Abs	Abs	Abs	Abs/Abs
W202		Em	Abs		Abs/Abs	W300	Em	Em	Abs		Abs/Abs	W472	Em		Abs	Abs	Abs/Abs
W203	Em		Abs		Abs/Abs	W301				Em	Abs/Em	W483		Em		Em	Em/Em
W205			Abs	Em	Abs/x	W306	Em	Em	Abs		Abs/Abs	W484		Em	Abs	Abs	x/Abs
W207	Em	Em	Abs		Abs/x	W307	Em		Abs		Abs/Abs	W494		Em	Em		Em/x
W210	Em			Abs	Abs/x	W310	Em				Abs/x	W496	Em		Abs		x/x
W213		Em	Abs		Abs/x	W311	Em		Abs	Abs	Abs/x	W500				Em	Em/Em
W221	Em		Abs		Abs/x	W313		Em	Abs	Abs	Abs/Abs	W503	Em		Em	Em	Em/Em
W227	Em		Abs	Abs	Abs/x	W322	Em		Abs		Abs/x	W504		Em	Abs	Abs	Abs/Abs
W232		Em			Abs/x	W323	Em		Abs		Abs/Abs	W525		Em			x/x
W235	Em		Em	Em	Em/Em	W336		Em	Abs	Abs	Abs/Abs	W536		Em		Abs	Abs/Abs
W243	Em		Abs		Abs/Abs	W339		Em	Abs		x/x	W601	Abs				Abs/Em
W245		Em	Em		Em/x	W351	Em		Abs	Abs	Abs/Abs	W611		Em			x/x
W251	Em		Abs		x/Abs	W371	Em		Abs		Abs/Abs	W617		Em			Abs?/x
W262	Em		Abs		x/x												

H93 = Hillenbrand et al. (1993); W97 = de Winter et al. (1997); H01 = Herbig & Dahm (2001);
E05 = Evans et al. (2005); M07 = this study (slitless/slit)

We note that almost all the spectra exhibit a narrow emission-line component onto the core of H line profiles with a Full Width at Half Maximum (FWHM) close to the spectral resolution. This component is due to the ambient nebulosity, which also produces many other nebular lines visible in the spectra, such as [SII] and [NII] lines.

3. Results

3.1. Comparison between WFI and VLT-GIRAFFE spectroscopy in NGC 6611

In Fig. 2, we compare the spectra obtained in the WFI slitless spectroscopic mode and the VLT-GIRAFFE high resolution spectroscopy. In Fig. 2-left, we show the example of the star W483 with a "true" circumstellar emission line in Hα, visible with the two instrumentations. We also show in Fig. 2-right the star W371, a Be star according to Hillenbrand et al. (1993). No emission is however detected with the WFI-spectro for this star. With the VLT-GIRAFFE observations, we found only a nebular emission (small FWHM) and no circumstellar emission.

Finally, in Table 1 we compare the ELS found in NGC 6611 depending on the techniques and studies. The presence of strong nebular emission could explain the high number of *false* Be stars previously observed in this cluster with low resolution slit or fibre spectroscopy by several authors.

3.2. Spectroscopy of circumstellar ELS

With the VLT-GIRAFFE, we found 9 *true* ELS: 3 of them (WFI[N6611]017, W031, W080) are newly detected ones; 6 of them (W235, W301, W483, W500, W503, W601) preselected from previous studies (Hillenbrand et al. 1993; de Winter et al. 1997; Herbig & Dahm 2001) or recently discovered (Evans et al. 2005; Alecian et al. 2008) are confirmed.

We measure the equivalent width of the Hα emission line (EWα) as a first clue to determine their nature. Note that several new ELS show faint EWα, which could only be detected with a large telescope such as the VLT and a high spectral resolution such as the one on the HR15N setting of GIRAFFE. Results are given in Table 8. EWα have been corrected from the nebular contribution, in the same way as we proceeded for Be stars in the Magellanic Clouds (see Martayan et al. 2006b). The Hα line of the 9 ELS with circumstellar (CS) emission observed with VLT-GIRAFFE is shown in Figs .10 to .19. The WFI spectrum is also shown when available. Unfortunately, the slitless spectrum was saturated for W235, W503 and W601. The stars WFI[N6611]017, W235, W483, W500, and W503 also show a CS emission in the Hβ line.

3.3. Fundamental parameters of OBA and ELS stars

As in Martayan et al. (2006a, 2007) we make use of the GIRFIT least-square procedure (Frémat et al. 2006) to derive the fundamental parameters: effective temperature ($T_{\rm eff}$), surface gravity ($\log\ g$), projected rotational velocity ($V \sin i$), and radial velocity (RV). This procedure fits the observations with theoretical spectra interpolated in a grid of stellar fluxes computed with the SYNSPEC programme and from model atmospheres calculated with TLUSTY (Hubeny & Lanz 1995,and references therein) or/and with ATLAS9 (Kurucz 1993; Castelli et al. 1997). The grid of model atmospheres we used to build the GIRFIT input of stellar fluxes was obtained for the metallicity of the Milky Way (MW). For a more detailed description of the grid of model atmospheres and of the fitting criteria we adopt in the GIRFIT procedure, we refer the reader to Sect. 3 of Martayan et al. (2006a). Resulting fits and the corresponding residuals obtained for the CS ELS are depicted in Figs .10 to .19 (upper panel). In the residuals several structures appear: Fe II emission lines at 4233, 4173-78, and 4385 Å are present in W235 and W500. However, in W483 and W503 false structures appear, e.g. false P Cygni lines, probably due to the uncertainty on RV used in the fit (RV is determined at $\pm$10km s^{-1}).

Finally, we determine the spectral classification of each star with a method based on the fundamental parameters. The calibration we established to estimate these spectral types is described in Martayan et al. (2006a).

Early-type stars are listed in Table .2, sorted by ID number from the literature or Simbad (WXXX, from Walker 1961) or from our WFI-catalogue (WFI[N6611]XXX). The fundamental parameters $T_{\rm eff}$, $\log\ g$, $V \sin i$, and RV obtained by fitting the observed spectra, as well as the spectral classification deduced from $T_{\rm eff}$–$\log\ g$ plane calibration (CFP determination Martayan et al. 2006a) are reported in this Table. The classification provided by Evans et al. (2005) for some of our targets observed with the same instrumentation is also given.

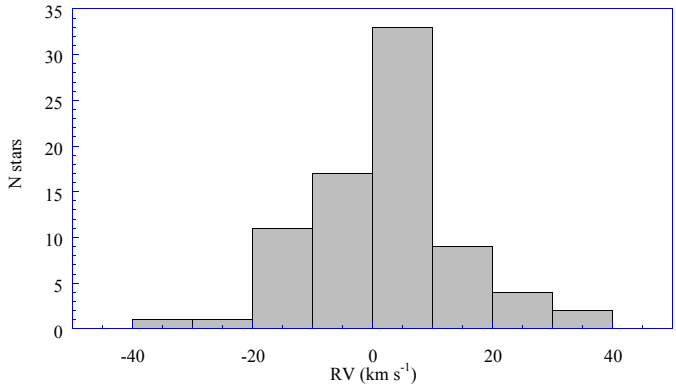

Fig. 4. Distribution of stellar radial velocities. The typical error-bar is $\pm$10 km s^{-1}.

We compare the fundamental parameters determined by Dufton et al. (2006) with ours for the 14 stars we have in common ((this study - Dufton et al.)/this study $\times$ 100 in percents). We found on average a difference of 0.1% (average: 19946 K) for $T_{\rm eff}$, 4.1% (average: 4.1 dex) for $\log\ g$, and 9.5% (average: 179 km s^{-1}) for $V \sin i$.

We note that the distribution of RV shown in Fig. 4 is similar to the one determined by Evans et al. (2005) for this cluster.

To determine whether the stars are members or not of the open cluster NGC 6611, we used the membership probabilities from Tucholke et al. (1986) and Belikov et al. (1999). We considered that the star is member of NGC 6611 if the average of the 2 membership probabilities is higher than 50 % or the probability is higher than 50 % if only one of the two probabilities is present. The membership probabilities are reported in Table .5 and are used in the following sections and figures.

To derive the luminosity, mass, age, and radius of OBA stars from their fundamental parameters, we interpolated in the HR-diagram grids (Schaller et al. 1992) calculated for MS stars without rotation at the solar metallicity (Z = 0.020). The obtained luminosity, mass, radius, and age of most OBA stars of the sample are given in Table .3. The masses are in good agreement with the calibration of Huang & Gies (2006) for B-type stars at the ZAMS. The position in the HR diagram of each observed star, members of the cluster and non-members, is shown in Fig. 5.

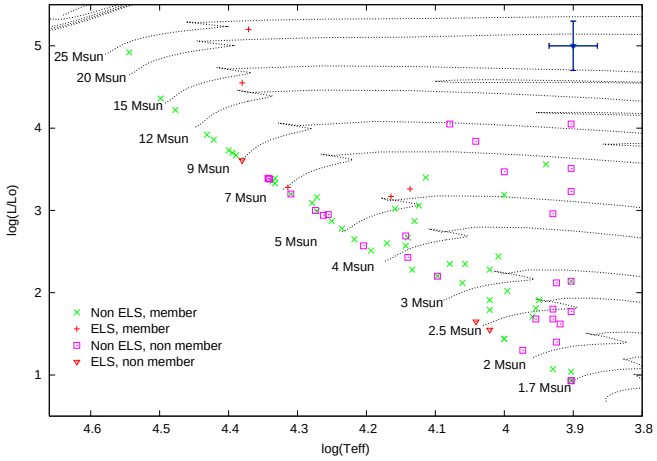

Fig. 5. HR diagram. Red '+' are for the ELS members of NGC 6611, red triangles are for the ELS non-members of the open cluster. Green 'x' are for the non-ELS members of NGC 6611, and the pink squares are for the non-ELS non-members of the open cluster. The tracks for Z=0.020 come from Schaller et al. (1992). The star is considered as member of the cluster if the average of membership probabilities is higher than 50% or the membership probability higher than 50 % in case of only one is present, for more detail about the membership see Sect. 3.3.

This figure shows that the most massive non-emission B-type stars (5$<\ M/M_{\odot} \leq$25) are located at the ZAMS,

while most of the less massive stars ($2 \leq M/M_{\odot} \leq 5$) are above the ZAMS. The latter may appear evolved and too old for this region, but are in fact probably PMS stars, which are going to reach the ZAMS.

3.4. Binaries

We identify binaries in our sample: (i) by cross-correlation with the study of Duchêne et al. (2001) of visual binaries detected with adaptive optics; and (ii) by using the radial velocity discrepancies between our measurements and those of Evans et al. (2005). We define two categories, first with RV discrepancies between 10 and 15 km s^{-1}, second with RV discrepancies higher than 15 km s^{-1}.

We confirm the binary nature of W025, W125, W175, W188, W243, W267, W275, W299, W313, W343, W364, W400, W472, and W536 already detected by Duchêne et al. (2001) or Evans et al. (2005). Moreover, we detected 8 other possible binaries: W161, W239, W409, W444, W469, W473, W503, and W582. Among them, W503 is an ELS and W343 is a SB2 with 2 B-type components. The indications of binarity from spectroscopy are reported in Table .2.

Evans et al. (2005) found in their sample a proportion of ∼10% of binary B-type stars, based on the RV scatter in their observations. We find a ratio of binaries equal to 22% of our entire sample and 27% of the B-type objects, which is in good agreement with the proportion reported by Porter & Rivinius (2003). The ratio of binaries among our limited sample of A-type objects is equal to 8%, certainly underestimated.

We searched for lightcurves for the binaries as well as the ELS in our sample in the ASAS database (Pojmanski et al. 2005). Unfortunately when photometry is found, the time-sampling, time coverage, and the quality of the data do not allow to study reliably the potential periodicity of the variations. The best lightcurve is the one of W503, which shows 3 eclipses without possibility to find a periodicity.

3.5. Infrared study

We search for infrared (IR) excess in each star, which could be attributed to a circumstellar environment. First, with the Herbig (1975) calibration of interstellar extinction based on the equivalent widths of diffuse interstellar absorption bands at 4430 Å and 6613 Å, we determine the local E(B-V) for each star with or without emission lines. We also consider the two stars W245 and W494 reported as ELS by Herbig (1975) and confirmed by our WFI spectra but for which no GIRAFFE spectra are available. For these 2 stars we use a mean E(B-V) value.

Then, we search for their J, H, K-band magnitudes in the 2MASS catalogue and 3.6, 4.5, 5.8 and 8.0 μm magnitudes in the GLIMPSE archive of SPITZER (release: spring07, 06/12/2007). We determine the colour indices $(J\text{-}H)_0$ and $(H\text{-}K)_0$ (see Table .4) as well as the colour indices $(3.6\text{-}4.5)_0$ and $(5.8\text{-}8.0)_0$. The 2MASS colour-colour diagram is shown in Fig. 6. We marked off in this graph the area defining classical Be stars and Herbig Ae/Be stars with a strong IR excess, as defined by Hernández et al. (2005).

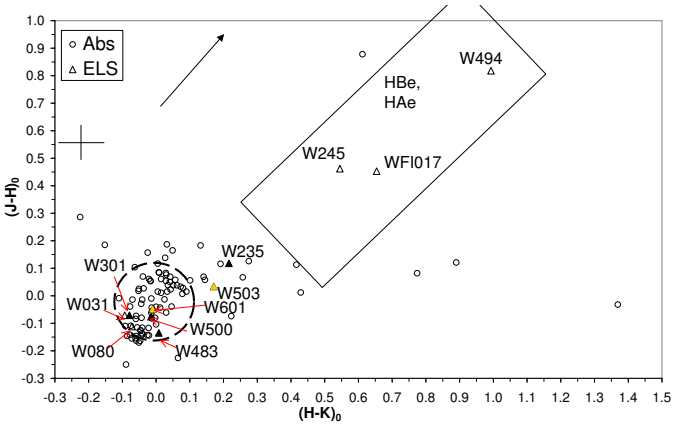

Fig. 6. Colour-coulour diagram based on 2MASS magnitudes corrected from the local extinction for the stars observed in NGC 6611 and in the Eagle Nebula. The large box shows the area of Herbig HAe/Be stars and the small dashed ellipse shows the area of classical Be stars, according to Hernández et al. (2005). Note that several Herbig Ae/Be and PMS stars can exist in the area of classical Be stars. ELS are indicated by a triangle, filled in black if the star is a member of NGC 6611, filled in yellow if the membership is uncertain, and empty if the star is not a member. WFI017 is for WFI[N6611]017. The open circles are for non-ELS (without indication of the membership to NGC 6611). The cross in the top left corner indicates the mean error, and the arrow indicates the reddening vector. For more details about the membership see Sect. 3.3 and Sect. 4.

The figure 6 shows that several stars have a strong IR excess in 2MASS and lie in or close to the area of PMS stars or Herbig Ae/Be. This is the case for the ELS WFI017, W245, and W494, which fall into the HAeBe area. Note that Herbig Ae/Be stars could also have weak IR excess and fall in the classical Be star area as it could be shown by using data from Vieira et al. (2003) and The et al. (1993) for example. Note also that between the area of MS stars and HAeBe, classical Be as well as HAeBe could also lie as it could be shown by using data from Vieira et al. (2003) and The et al. (1993) for HAeBe and from Currie et al. (2007) for classical Be stars. However, the star W235 seems to have an IR excess stronger than those of classical Be stars and must be considered as an HBeAe. The excess for W503 is probably due to the disk of the binary. For the other ELS (W031, W080, W301, W483, W500, W601), this Fig. 6 indicates a possible MS status. Note that several non-ELS have also a strong IR excess, which indicates a possible PMS nature. This is the case for W026, W299, W568, and 4 others with a very strong excess: W307, W409, W596, W627, W633. Note that the

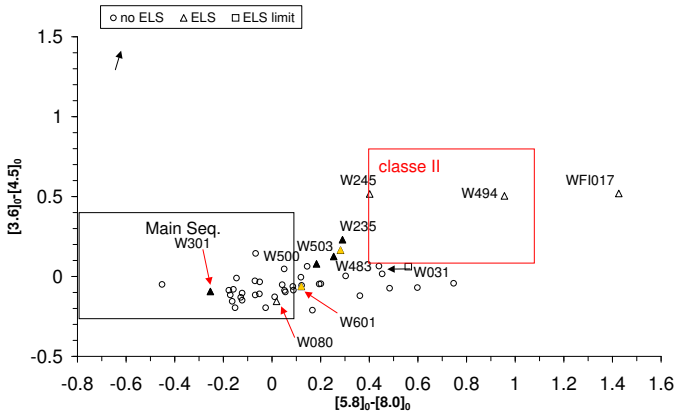

Fig. 7. Colour-coulour diagram from IRAC/SPITZER magnitudes corrected from the local extinction for the stars observed in NGC 6611. The red box is the area of class II objects following Allen et al. (2004). The black box is the area of MS stars. Note that the boxes are not dereddened here. ELS are indicated by a triangle, filled in black if the star is a member of NGC 6611, filled in yellow if the membership is uncertain, and empty if the star is not a member. Non-ELS are indicated with a circle (without indication of the membership to NGC 6611). W031, which does not have a measured magnitude at 8.0 μm but only the limiting magnitude of the GLIMPSE archive is noted with a diamond. Note that its location is a limit and could move to the left. The arrow (in the top left corner) indicates the reddening vector. For more details about the membership see Sect. 3.3 and Sect. 4.

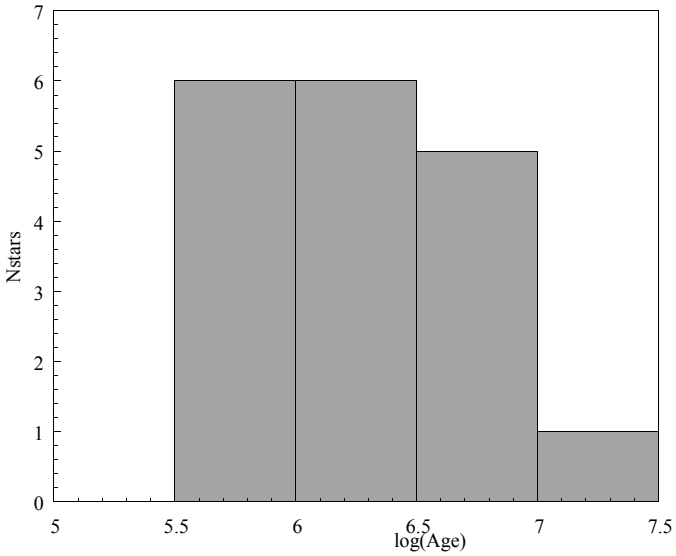

Fig. 8. Distributions of stellar ages for MS members of NGC 6611.

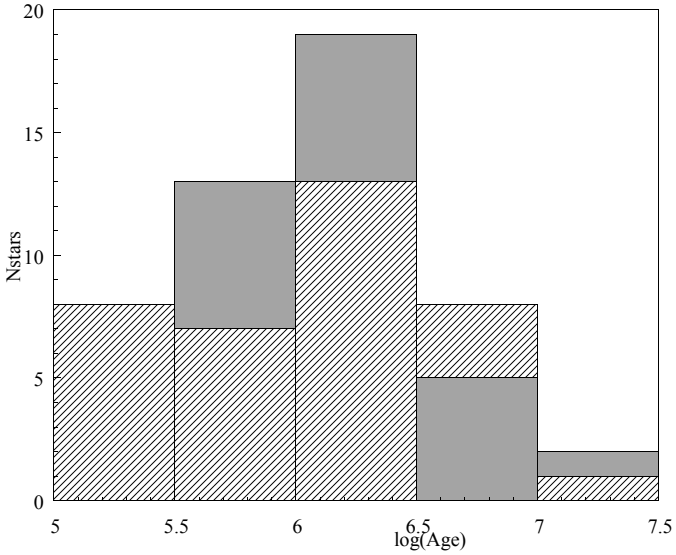

Fig. 9. Distributions of stellar ages for PMS (cross-hatched bars) + MS (filled grey bars) members of NGC 6611.

strong reddening of W299 and the medium excess of W400 could also be explained by their binary nature.

We also used the SPITZER colour-colour diagram to investigate the nature of the ELS stars (see Fig 7). In this graph the class II area, attributed to young stars with an accretion disk (PMS stars) as defined by Allen et al. (2004), is indicated as well as the MS area. The star W494 falls in the class II area, W245 is at its limit. According to the lower limit of its $(5.8\text{-}8.0)_0$ colour index, the ELS star W031 could also be at the limit of the class II area.

The star WFI017, close to the centre of the HAeBe area in the 2MASS colour-colour diagram falls outside the PMS star domain (class II area) in the SPITZER colour-colour diagram, sharing the domain of very young objects (class I area, Allen et al. (2004)); this optical source might then be a young class II source projected onto a locally dense cloud which could explain its abnormal excess in the $(5.8\text{-}8.0)_0$ colour index. According to Indebetouw et al. (2007), WFI17 has an accretion disk. W235, W503, W500, W483 have a mid-IR excess and fall in the area between MS and class II stars. W301 seems to be clearly a MS star, while W080 and W601 are at the edge of MS area to intermediate area between MS and class II areas. The non-ELS W026, W239, W400, W444, W473, W520, W536 have also a strong infrared excess and are close to the area of class II.

As it could be shown by using data from the literature (see above for the references) for HAeBe and for classical Be stars CBe as well as HBeAe and PMS stars could fall in the intermediate area between class II and MS. See also Sicilia-Aguilar et al. (2006) who shew that stars with weak emission could also fall in MS and in the intermediate area between class II and MS.

The indication of infra-red excess is reported for each star in Table .5.

3.6. Age of the cluster NGC 6611

We obtained the age of NGC 6611 by using gaussian fitting values of the age-distributions of the stars and PMS objects belonging to this cluster, as shown in Figs. 8 and 9.

For this purpose, we only take into account the stars that have their average membership probability higher than 50% (see Table .5 and Sect. 3.3). We also determine the age by merging the PMS objects with MS stars.

We identified the potential PMS and MS stars (see Table .5) by using indications provided by IR data or from the fact that their age derived from the MS tracks seems too old for the members of the cluster. Then, we derive the age of PMS stars by interpolation in the PMS tracks given by Iben (1965) and/or from Palla & Stahler (1993), while for MS stars, as in Martayan et al. (2006a, 2007), we determine the age of each star by interpolation in HR tracks of MS stars (Schaller et al. 1992). The distribution of stellar ages of MS stars in the cluster is displayed in Fig. 8 and for the PMS+MS in Fig. 9. The age finally retained for each star of the global sample is reported in Table .5. Then, we consider that the age of the cluster has to be derived only from the MS stars members of the cluster, i.e. the more massive stars, which are close to the ZAMS, or from the MS stars with PMS objects merged. We find log(age NGC 6611)=6.25±0.30 (i.e. 1.78 Myears) from MS stars, and 6.08 ±0.25 (i.e. 1.20 Myears) from MS+PMS stars in good agreement with the log(age)=6.0–6.5 recently determined by Dufton et al. (2006) or with log(age)=6.11 (1.3 Myears) by Bonatto et al. (2006). Note that the age determined here is younger than the previous estimates from the photometric studies (6.882, see WEBDA).

Table 6. Comparison of the mean rotational velocities for PMS and MS stars. The mean $V \sin i$, the median $V \sin i$, and the statistical error are given in cols. 3, 4, and 5, respectively. In the upper part of the table, we first give the values for the whole PMS or B-type PMS samples, and then with the binaries removed from the samples. In the lower part of the table, we give the same statistics as in the upper part but for the MS stars. Note that only the stars with a reliable status are kept here.

Sub-sample	Number	$V \sin i$ in km s^{-1}			
	of objects	Aver.	Med.	error	D06
All PMS	32	169	155	±20	
PMS B-type	18	213	201	±25	187
PMS B-type - bin	12	238	236	±31	
All MS	26	162	157	±15	
MS B-type	23	165	183	±17	132
MS B-type - bin	18	183	199	±18	

D06: Dufton et al. (2006, their Table 6)

3.7. Rotational velocity statistics

It is very difficult to compare the rotational velocities of the objects in- or outside of NGC 6611 due to the small number of stars in these sub-samples. Moreover, the membership probability varies highly from a study to an other. It is nevertheless interesting to statistically study the rotational velocities of MS and PMS stars, irrespective of their membership. To increase the number of objects in the sub-samples, we thus merge the PMS objects in- and outside of the cluster and we do the same for the MS stars. We remove, in a second step, the binaries. Note that only the stars with a reliable status (MS or PMS) are kept here (see Sect. 4.3 and Table .5). We then compare the mean and median stellar rotational velocities of the sub-samples of PMS and MS stars as well as of B-type PMS and MS objects. The results are given in Table 6.

Table 7. Ratios of the mean or median rotational velocities for the B-type PMS and MS objects, with or without binaries included in the sample.

	$\frac{MSB}{PMSB}$	$\frac{MSB-bin}{PMSB-bin}$
Average	0.77	0.77
Median	0.91	0.84

The comparison shows that B-type PMS objects rotate with a higher rotational velocity than MS stars. The trend of these velocities is in fair agreement with the trend of rotational velocities determined by Dufton et al. (2006,Table 6) as shown in Table 6. This result could be explained by the fact that the stars at the ZAMS undergo a first contraction with a redistribution of their internal angular momentum, generating a decrease of their rotational velocity. Note that, in the theoretical diagrams by Meynet & Maeder (2000), the rotational velocity decreases by ∼20% during this contraction. Here we find on average for B-type stars a decrease of 18% (i.e. ratio $\simeq$ 82%) as shown in Table 7, in excellent agreement with the theoretical calculation. Note that, this result is also important to constrain the models of the stellar evolution with rotation from PMS phase to MS.

The fact that we find stellar rotational velocities higher for the PMS candidates than for the true MS stars supports our conclusion that these objects are actually PMS stars and not evolved MS stars. Due to stellar winds (see Meynet & Maeder 2000), the stellar rotational velocities of evolved stars would be lower than non-evolved stars or PMS stars.

4. Discussion on the nature of the stars

4.1. True circumstellar ELS

In this section we discuss the nature of each ELS observed in NGC 6611 and its surrounding field. We use information reported in previous sections and summarized in Table 8. Note that the masses of the following stars (W503 excluded) are in the range of masses for PMS stars (M<15M$\odot$ Iben 1965).

– **W245 and W494:** We confirm the result of Herbig & Dahm (2001) about W245 and W494, which are also found as ELS with our WFI observations. Their infrared excess indicate that they are Herbig Ae/Be

Table 8. Parameters and indications for true circumstellar ELS. In col. 11 the presence of infrared excesses based on 2MASS (2M) and on SPITZER (SPI) data are indicated. In col. 12, the membership (MP) to the open cluster NGC 6611 is indicated: y (for reliable membership), u (for uncertain membership), and n (for non-membership). In the last column, the nature of the ELS is given as well as the presence of an accretion envelope (class I protostar), or whether the star is a MS object or at the ZAMS.

Stars	EWα (Å)	$T_{\rm eff}$ K	log g dex	$V \sin i$ km s^{-1}	CFP	$M/M_{\odot}$	age MS Myears	age PMS Myears	E[B-V]	IR excess 2M/SPI	MP	age kept Myears	Nature
WFI17[0]	15	9600	4.2	169	A1V	2.3	239	3	0.742	yes/yes	n	3	HAe, class I
W031	2	9000	3.7	156	A2IV	2.7	432	1	0.898	no/yes?	n	1	probably HAe
W080	undef[1]	24000	4.3	183	B1V	8.9	0.5	0.1	1.866	no/no	n	0.5	possible He-strong, ZAMS
W235	>60[2]/70[3]	24000:	3.5:	482:	B1IV	13.9:	12:	0.02	0.978	yes/yes	y	0.02	HBe
W301	2	20600	4.2	115	B2V	7.0	7	-	0.905	no/no	y	7	CBe, MS
W483	11/11[3]	14600	3.6	186	B3IV	5.4	79	0.1	0.747	no/yes	y	0.1	HBe
W500	13/13[3]	13700	3.4	289	B5IV	5.4	85	0.12	0.684	no/yes	y	0.12	HBe
W503	11/17[3]	23500:	3.0:	236:	B1III	21.7:	7:	0.02	0.687	yes?/yes	u	0.02	MS?, bin
W601	undef[1,4]	22500	4.0	190	B1V	10.2	-	0.016	0.691	no/no	u	0.016	He-strong, ZAMS
W245	-	-	-	-	A0[5]	-	-	-	-	yes/yes	n	-	HAeBe
W494	-	-	-	-	B[5]	-	-	-	-	yes/yes	n	-	HAeBe

[0]: WFI17 is written for WFI[N6611]017; [1] : EW undefined, P Cygni profile, very weak emission; [2]: Hα saturated;
[3]: EW measured in spectra from Evans et al. (2005); [4]: Fundamental parameters from Alecian et al. (2008), [5]: from Simbad.

stars. However, W245 and W494 are not member of NGC 6611 but lie in the ambient star-formation region of the Eagle Nebula and as WFI017 (see below) are representative to its PMS (A, B)-population.

– **WFI017:** The emission of WFI[N6611]017 is moderate and the spectrum does not display any Fe II permitted and forbidden emission lines. However, this star shows a strong IR excess, in particular in the SPITZER colour/colour diagram, like very young objects. This large IR excess is compatible with the one of HAeBe stars. This star is not a member of NGC 6611 and the age for this star derived from MS tracks is very old (239 Myears). This old age is not compatible with a PMS status. In fact, this star is representative of a PMS population not member of NGC 6611 itself but member of the surrounding star-formation region of the Eagle Nebula, as shown by Indebetouw et al. (2007,private communication). Thus the true age of this star was determined with PMS tracks (3 Myears). In conclusion, we propose this star as a possible HAe star.

– **W031:** The Hα emission is weak. W031 has a potential IR excess in the SPITZER colour/colour diagram, even if the magnitude at 8 μm is not well defined, which favours a PMS status. The star is not a member of NGC 6611, and its RV indicates a field star. The age of W031 (432 Myears) is very old, and except if the star is a foreground star, its age is not compatible with the star-formation region of the Eagle Nebula. Moreover Indebetouw et al. (2007) found two PMS objects very close to W031. With these indications, it seems that W031 could be more probably a HAe than a CBe, and its age is probably 1 Myear.

– **W235:** The EW of the Hα emission line is 70 Å. This value is unusual for CBe, but is often seen in Herbig Ae/Be stars. The 2MASS and SPITZER diagrams also indicate a probable Herbig star. This star is clearly a member of NGC 6611 and its RV is compatible with the NGC 6611 RV distribution of stars. Its age from HR tracks (12 Myears) is too old for NGC 6611. This star is already known as a HBe star and we thus confirm its nature.

– **W301:** The Hα emission is weak. The 2MASS and SPITZER diagrams indicate a MS star. The star is a member of the cluster and its RV is compatible with the NGC 6611 RV distribution of stars. Its MS age determined is compatible with the age of the cluster and its evolutionary status ($\frac{\tau}{\tau_{MS}}$=16%) falls in the area of classical Be stars. We thus propose W301 as a classical Be star.

– **W483:** The Hα emission is moderate. The infrared excess found in SPITZER diagram cannot settle the status of this star, we have to consider the membership of the star to NGC 6611 and to compare the ages. The star is a member of the cluster and its RV is compatible with the NGC 6611 RV distribution of stars. Its MS age determined is too high (79 Myears) as compared to the age of the cluster. We thus confirm W483 as a HBe star.

– **W500:** The emission in Hα is moderate. As for W483, the infrared study cannot help to conclude on the nature of this star. However, the star is a member of the cluster and its RV is compatible with the NGC 6611 RV distribution of stars. Its MS age determined is too high (85 Myears) as compared to the age of the cluster. We thus confirm W500 as a HBe star.

– **W503:** The Hα emission is moderate. The profiles of the Hα, Hβ and Hγ emission lines are asymmetric and show 2 violet (V) and red (R) peaks with V>R, as often observed in Herbig Ae/Be stars. The infrared study indicates an infrared excess but cannot help to conclude on the nature of this star. The membership of this star to NGC 6611 is uncertain (94% and 40 %

from Tucholke et al. (1986) and Belikov et al. (1999) respectively) and the RV cannot be used due to the binarity of this system. For this star, the emission lines profiles as well as the infrared excess can be interpreted by a mass-transfer binary, in which the line emission arises from an accretion disk. The mass of this star was estimated to $\sim$22M$\odot$, too high for HBe/Ae, but due to the binarity of this star, the mass determined is not reliable. Note that this star is a binary as many Herbig Ae/Be stars. However, we propose W503 as a possible MS star.

– **W601:** This star and W080 have common properties: their Hα profile is P Cygni-like and their IR excess is very weak. Their fundamental parameters are very similar. The membership of W601 to NGC 6611 is uncertain (93% and 43 % from Tucholke et al. (1986) and Belikov et al. (1999) respectively). This star is an He-strong star and hosts a magnetic field (Alecian et al. 2008) as found in about 8% of Herbig Ae/Be stars and is proposed as an Herbig Be star close to the ZAMS by Alecian et al. (2008). In fact, if this star is not a member of NGC 6611 itself, as WFI017, W601 is a member of the surrounding star-formation region of the Eagle Nebula.

– **W080:** As indicated above, its spectral profiles and IR excess are similar to those of W601. W080 is not a member of NGC 6611 but is a member of the ambient star-formation region of the Eagle Nebula, while its RV is not different from the average RV of the RV distribution in NGC 6611. Moreover, W080 seems to be very close to a new young open cluster, which undertook to emerge to the ambient nebula (see Fig. .3). Its age (0.5 Myear) is compatible with this star-formation region. W080 could be either a classical Be star or a Herbig Be star at the ZAMS, whose disk has been blown away by the stellar wind. Consequently, the Hα line may exhibit a P Cygni profile as the HAeBe star AB Aur and according to Finkenzeller & Mundt (1984). However, we found that the NLTE models do not reproduce correctly the HeI lines in the LR2 domain as shown in Fig. .12-top. We also compare in Fig. .13 the HeI 6678 Å line to the NLTE models for W080 and for W601, already known as a magnetic He-strong star. W080 and W601 show similar line profiles and similar fundamental parameters, the NLTE models are not able to reproduce their HeI line profiles. As W601 is already known as a magnetic He-strong, we propose W080 as a potential new He-strong star. Moreover, this star lies in an area where the polarisation measured by Bastien et al. (2004) is large and of interstellar origin, a very good grain alignement is needed, probably calling for a correspondingly large local interstellar magnetic field in the parent molecular cloud, near W080.

4.2. Previously suspected "Be" stars

The other potential Be stars from the literature are seen as non-ELS in our data but often with strong nebular lines. See the WFI slitless and VLT-GIRAFFE spectra examples in Fig. 2 for the star W371, which exhibits strong nebular lines and no circumstellar line in Hα. This is the case for the stars listed in Table 1. The stars W138, W202, W203, W207, W210, W213, W221, W227, W243, W251, W267, W273, W281, W297, W299, W300, W306, W307, W311, W313, W322, W323, W336, W351, W371, W374, W388, W389, W396, W400, W455, W469, W472, W484, W504, W536, and W617, are non-ELS in our data and we confirm the status of non-Be stars as indicated by Herbig & Dahm (2001); Evans et al. (2005). W205 is found as an 04Vf by Evans et al. (2005) but do not display sufficient emission to be seen in our WFI data.

We infirm the nature of Be stars for the stars W181, W198, W232, W310, W617, which have spectra in absorption in our data.

4.3. Non-ELS

To determine if the star is a MS star or a PMS star, we used the same criteria as for the ELS. First, if the star has a strong infrared excess compatible with the area of PMS objects, we consider then the star as a PMS. Second, if the star is member of NGC 6611 and its MS age too old for the youth of NGC 6611, we consider that the age is not the true one, and the star must be considered as a PMS object and its age was interpolated in PMS tracks. Third, if the star has no infrared excess and if its membership to NGC 6611 is uncertain, we considered in general by default that the star is a potential MS star (noted as "MS") even if its age seems too old for the ambient star-formation region (noted as "MS?"), while the stars with several hundreds of Myears are noted as "PMS?". We also use indications about the nature of the stars from previous studies of Walker (1961); Tucholke et al. (1986); Ogura et al. (2002); Indebetouw et al. (2007). Note that all non-ELS considered here as PMS objects have masses lower than $8M_{\odot}$, in agreement with the masses expected for this kind of objects (M<$15M_{\odot}$ Iben 1965). All the details about each star are given in Table .5.

5. Conclusion

Thanks to our observations with 2 different instrumentations, the ESO-WFI in slitless spectroscopic mode which is not sensitive to the ambient nebula and the VLT-GIRAFFE fibre multiobjects high-resolution spectrograph, we were able to find a small number of true circumstellar ELS (in Hα) among the brightest population of the very young cluster NGC 6611 and the star formation region of Eagle nebula. With spectra obtained at the VLT, we were able to study accurately their nature: Herbig Ae/Be or classical Be star. We also conducted the same study for the other non-ELS. Finally, only 11 true

ELS with circumstellar or wind emission were found. The other previous potential Be stars from the literature are actually stars with a strong nebular emission pollution in Hα.

We determined the fundamental parameters for 85 stars and gave general information for several others. Among our sample of B-type stars, we found 27% of them as binaries. Concerning rotational velocities, we found that the B-type MS stars rotate 18% slower than B-type PMS objects, in good agreement with published theoretical models at the ZAMS. This value could be used to constrain the models currently developed for the stellar evolution with rotation from the younger (PMS phase) to the older ages (G. Meynet, private communication). With IR data, we found that the low-mass stars are mainly PMS stars without circumstellar emission.

We redetermined the age of NGC 6611, found equal to 1.2–1.8 Myears, in good agreement with recent estimates. With clues from spectroscopy, IR, HR ages, membership probabilities, RV, and evolutionary status, we found that: there is a MS population and a PMS population in NGC 6611 itself but also in the surrounding ambient star-formation region of the Eagle Nebula. Among the true circumstellar Hα ELS, we found that: WFI017, W245, W494, W235, W483, W500 are Herbig Ae/Be stars; W301 is a classical Be star, W503 a binary with an accretion disk, and W080 is a possible He-strong magnetic star like W601. This study confirms that the appearance of Be stars is mass- and age-dependent.

Acknowledgements. C.M. acknowledges Drs E. Bertin, E. Alécian, C. Catala, R. Indebetouw, G. Meynet, E. Puga, and C. Evans for their useful information for our study. This research has made use of the Simbad and Vizier databases maintained at CDS, Strasbourg, France, of NASA's Astrophysics Data System Bibliographic Services, and of the NASA/ IPAC Infrared Science Archive, which is operated by the Jet Propulsion Laboratory, California Institute of Technology, under contract with the National Aeronautics and Space Administration. C.M. acknowledges funding from the ESA/Belgian Federal Science Policy in the framework of the PRODEX program (C90290). We also acknowledge the anonymous referee for his very useful comments.

References

Alecian, E., Wade, G. A., Catala, C., et al. 2008, A&A, 481, L99
Allen, L. E., Calvet, N., D'Alessio, P., et al. 2004, ApJS, 154, 363
Baade, D., Meisenheimer, K., Iwert, O., et al. 1999, The Messenger, 95, 15
Bastien, P., Ménard, F., Corporon, P., et al. 2004, Ap&SS, 292, 427
Belikov, A. N., Kharchenko, N. V., Piskunov, A. E., & Schilbach, E. 1999, A&AS, 134, 525
Bertin, E. & Arnouts, S. 1996, A&AS, 117, 393
Bonatto, C., Santos, Jr., J. F. C., & Bica, E. 2006, A&A, 445, 567
Castelli, F., Gratton, R. G., & Kurucz, R. L. 1997, A&A, 318, 841
Currie, T., Balog, Z., Kenyon, S. J., et al. 2007, ApJ, 659, 599
de Winter, D., Koulis, C., The, P. S., et al. 1997, A&AS, 121, 223
Duchêne, G., Simon, T., Eislöffel, J., & Bouvier, J. 2001, A&A, 379, 147
Dufton, P. L., Smartt, S. J., Lee, J. K., et al. 2006, A&A, 457, 265
Evans, C. J., Smartt, S. J., Lee, J.-K., et al. 2005, A&A, 437, 467
Fabregat, J. & Torrejón, J. M. 2000, A&A, 357, 451
Finkenzeller, U. & Mundt, R. 1984, A&AS, 55, 109
Frémat, Y., Neiner, C., Hubert, A.-M., et al. 2006, A&A, 451, 1053
Herbig, G. H. 1975, ApJ, 196, 129
Herbig, G. H. & Dahm, S. E. 2001, PASP, 113, 195
Hernández, J., Calvet, N., Hartmann, L., et al. 2005, AJ, 129, 856
Hillenbrand, L. A., Massey, P., Strom, S. E., & Merrill, K. M. 1993, AJ, 106, 1906
Huang, W. & Gies, D. R. 2006, ApJ, 648, 580
Hubeny, I. & Lanz, T. 1995, ApJ, 439, 875
Iben, I. J. 1965, ApJ, 141, 993
Indebetouw, R., Robitaille, T. P., Whitney, B. A., et al. 2007, ApJ, 666, 321
Kurucz, R. L. 1993, VizieR Online Data Catalog, 6039, 0
Martayan, C., Frémat, Y., Hubert, A.-M., et al. 2006a, A&A, 452, 273
Martayan, C., Frémat, Y., Hubert, A.-M., et al. 2007, A&A, 462, 683
Martayan, C., Hubert, A. M., Floquet, M., et al. 2006b, A&A, 445, 931
Meynet, G. & Maeder, A. 2000, A&A, 361, 101
Ogura, K., Sugitani, K., & Pickles, A. 2002, AJ, 123, 2597
Palla, F. & Stahler, S. W. 1993, ApJ, 418, 414
Pasquini, L., Avila, G., Blecha, A., et al. 2002, The Messenger, 110, 1
Pojmanski, G., Maciejewski, G., Pilecki, B., & Szczygiel, D. 2005, VizieR Online Data Catalog, 2264, 0
Porter, J. M. & Rivinius, T. 2003, PASP, 115, 1153
Schaller, G., Schaerer, D., Meynet, G., & Maeder, A. 1992, A&AS, 96, 269
Sicilia-Aguilar, A., Hartmann, L., Calvet, N., et al. 2006, ApJ, 638, 897
The, P. S., de Winter, D., & Perez, M. R. 1993, VizieR Online Data Catalog, 410, 40315
Tucholke, H.-J., Geffert, M., & The, P. S. 1986, A&AS, 66, 311
Vieira, S. L. A., Corradi, W. J. B., Alencar, S. H. P., et al. 2003, AJ, 126, 2971
Walker, M. F. 1961, ApJ, 133, 438
Wallace, P. T. & Gray, N. 2003, User's guide of ASTROM
Zorec, J., Frémat, Y., & Cidale, L. 2005, A&A, 441, 235

Online Material

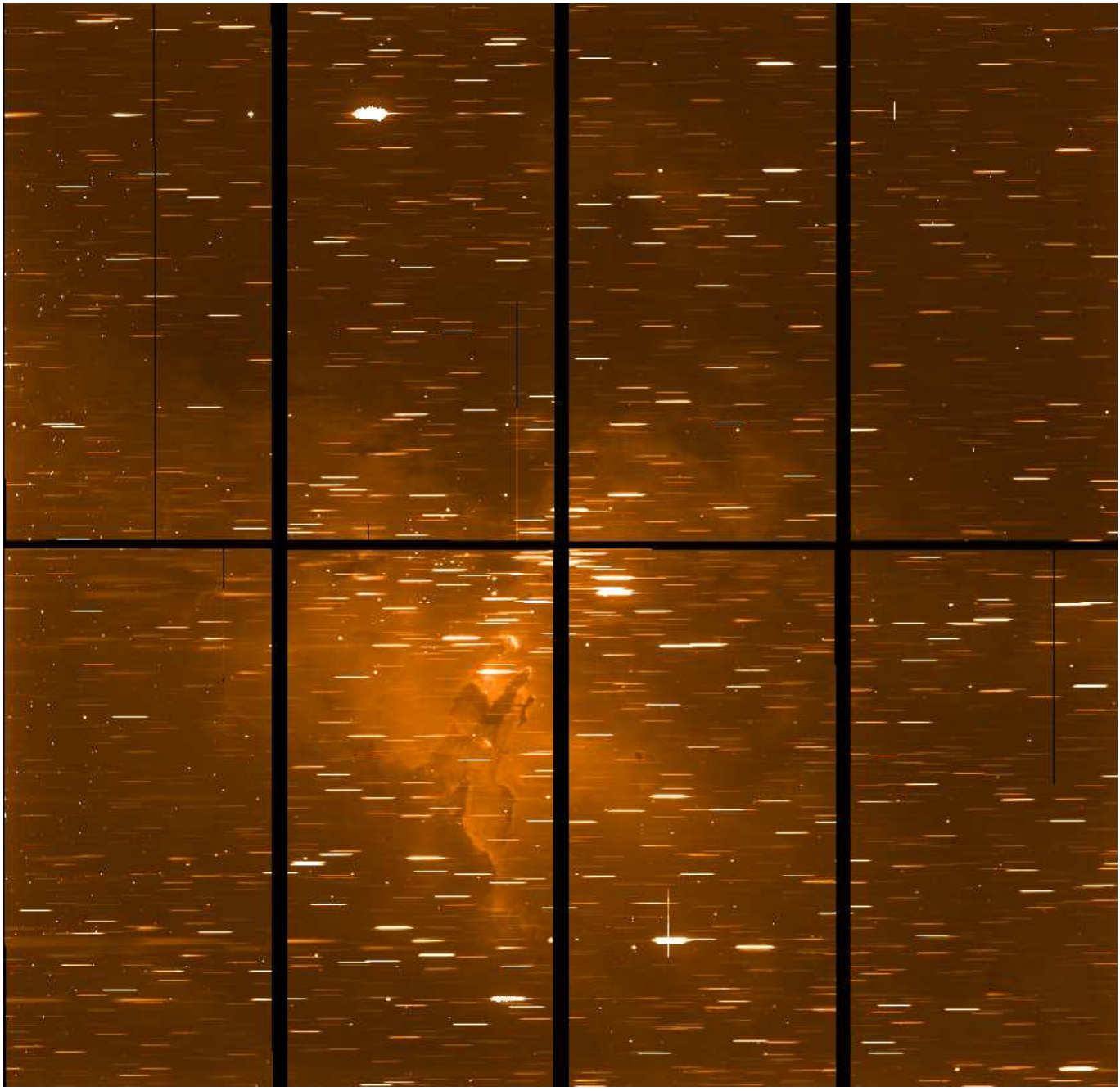

Fig. .1. Field of NGC 6611 obtained with the ESO-WFI in slitless spectroscopic mode with the filter RC (200 nm bandpass) centered on Hα. The center of this image is (α(2000) = 18h18min42s, δ(2000) = -13°46′57.6″), while the cluster lies at α(2000) = 18h18min48s, δ(2000) = -13°48′24″. North is at the top, East on the left. The stars appear as spectra. The diffuse background is due to the Hα emission line of the nebulosity. Note the elephant-trunk features, which correspond to shocks and often called "the pillars of creation". Also note the 0^{th} order of the spectra which appear as points in the image. The 2 images we obtained are combined in this figure.

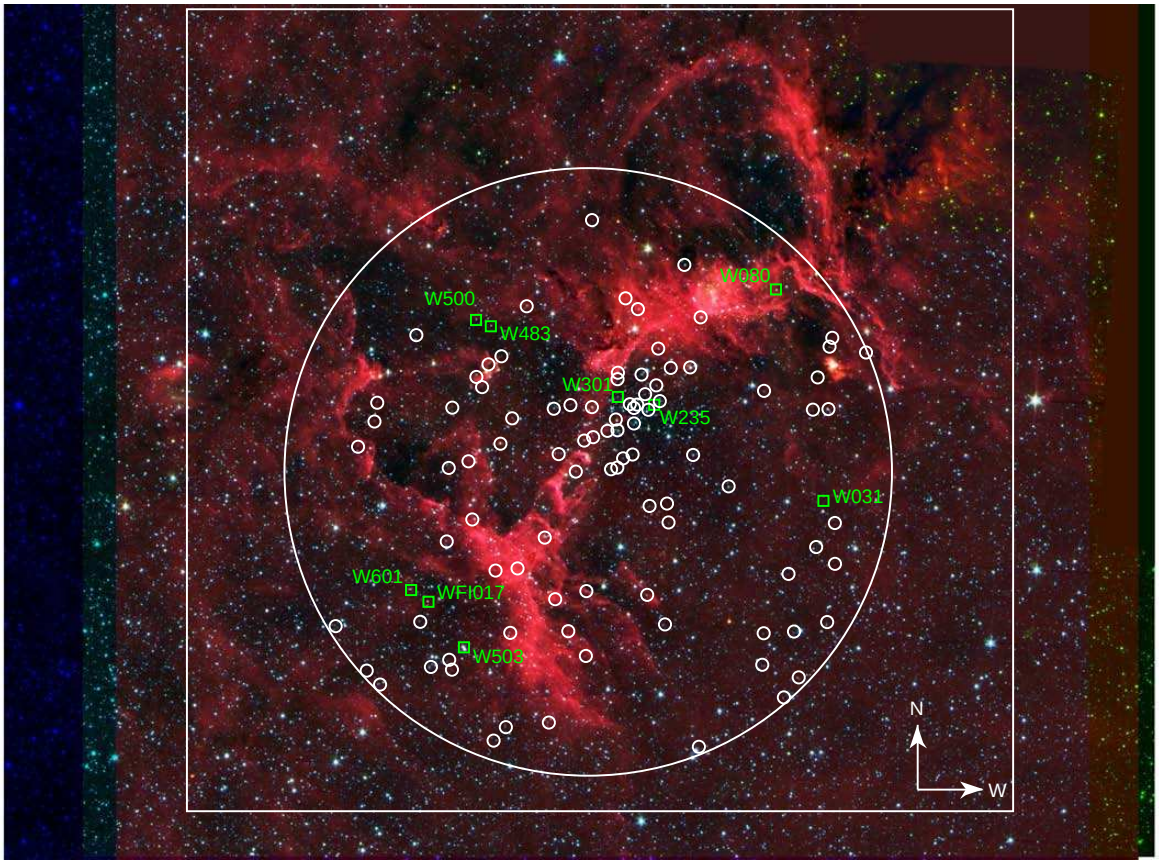

Fig. .3. Location of the stars observed with the VLT-GIRAFFE in the field of NGC 6611. The image is a RGB mosaic

Table .2. Fundamental parameters for stars observed with the VLT-GIRAFFE in the open cluster NGC 6611 and its surrounding field. In col. 1, the name of the object is given: WXXX from Walker (1961) or WFIXXX for WFI[N6611]XXX from our catalogue. The coordinates (α(2000), δ(2000)) are taken from the UCAC2 catalogue and are given in cols. 2 and 3. The magnitude V and colour index B-V are given in cols. 4 and 5. The signal to noise (S/N) ratio is given in col. 6. In cols. 7, 8 and 9 $T_{\rm eff}$ in K, log g in dex and $V \sin i$ in km s^{-1} are given. The errors in $T_{\rm eff}$ range from $\pm$500 to $\pm$1500K for spectrum with high to low S/N. The errors in log g range from $\pm$0.1 to $\pm$0.2dex for spectra with a high to low S/N. The errors in $V \sin i$ range from $\pm$10km s^{-1} to $\pm$30km s^{-1} for spectra with a high to low S/N. "CFP" corresponds to the spectral classification based on the fundamental parameters. Col. "obs" indicates with "Bew" if the star is detected as a Be star with the VLT-GIRAFFE spectra and with our WFI-spectro study. If "no L2" is written, there is no spectrum in this setting for the concerning stars (too bright). The 12th column "lit" gives indications from the literature and from Evans et al. (2005). The last column gives the radial velocity (error $\pm$10km s^{-1}) corrected from the heliocentric velocity.

Star	α	δ	V	B-V	S/N	$T_{\rm eff}$	log g	$V \sin i$	CFP	obs	lit.	RV
WFI[N6611]014a	18 19 06.043	-14 0 33.40	14.55	0.68	10	12000:	2.6:	348:	B8III-II:			28:
WFI[N6611]019	18 19 27.561	-13 57 40.56	14.56	0.70	15	11000	2.6	253	B9III-II			29
WFI[N6611]125	18 18 31.213	-14 0 48.48	13.94	0.65	15	8000	1.9	100	A7II			28
WFI[N6611]152	18 19 29.014	-13 48 27.81	13.71	0.71	30	8300	3.8	60	A4IV			28
W002	18 18 02.929	-13 44 34.77	10.56	0.35						no L2	_/B8III	
W018	18 18 08.181	-13 51 35.81	14.16	0.60	30	8000	4.3	117	A7V		A0sh/_	26
W024	18 18 08.647	-13 43 58.59	14.22	0.76	15	8000	3.6	68	A7IV-III			-21
W025	18 18 09.283	-13 46 54.55	12.93	0.98	80	24500	4.3	68	B1V	bin[1]	B0.5V/_	25
W026	18 18 09.110	-13 44 20.48	13.46	0.60	40	8900	3.7	33	A2IV			7
W035	18 18 11.348	-13 52 35.21	14.11	0.52	60	10000	4.5	275	A0V			4
W036	18 18 11.116	-13 45 36.35	13.40	0.61	25	8000	4.2	121	A7V		_/A7II	0
W041	18 18 11.921	-13 46 56.05	14.15	0.85	20	<8000			<A7			-6
W064	18 18 16.031	-13 53 41.58	13.74	0.53	30	8000	2.3	166	A7II			-9
W090	18 18 20.207	-13 46 09.70	11.73	0.38	175	14800	4.1	262	B4V		B3-5V/B5V	32
W125	18 18 26.196	-13 50 05.49	10.01	0.47						no L2, bin[2]	B1.5V/B1V+?	17:
W161	18 18 30.956	-13 43 08.23	11.29	1.05	130	35000	4.0	117	bin[3]?		O8V/O8.5V	10
W166	18 18 32.222	-13 48 48.06	10.37	0.57						no L2	O8.5/O9V	21:
W175	18 18 32.730	-13 45 11.88	10.09	0.84						no L2, bin[1,2]	O8.5/O5Vf+,SB2	
W188	18 18 33.719	-13 40 58.83	13.13	1.34	60	31500	4.3	239	B0V	bin[1]	B0V/_	-17
W194	18 18 36.380	-13 51 34.70	13.90	0.53	10				?			26
W201	18 18 36.973	-13 55 46.42	13.55	0.68	15	10000	2.7	48	A0III-II			14
W202	18 18 36.013	-13 45 13.12	14.40	0.96	55	12500	4.1	310	B7V		A0/_	13
W203	18 18 36.640	-13 50 48.02	14.19	0.47	35	9100	3.9	36	A2IV			-7
W223	18 18 37.865	-13 46 35.15	11.20	0.59	220	25100	4.4	95	B1V		B1V/_	5
W228	18 18 38.136	-13 44 25.47	13.51	0.93	70	21500	4.5	86	B2V		B2V/_	-3
W231	18 18 38.464	-13 45 56.22	12.71	0.75	135	24800	4.4	200	B1V		B1V/_	-1
W238	18 18 39.598	-13 50 54.00	13.37	0.67	50	9000	3.8	13	A2IV			-4
W239	18 18 39.993	-13 54 33.51	11.48	0.36	240	20400	4.3	95	B2V	bin[3]?	B1V/B1.5V	16
W243	18 18 39.810	-13 46 56.50	13.80	0.63	55	15600	4.4	30	B4V	bin[1]		38
W251	18 18 40.357	-13 46 18.08	13.34	0.69	110	20400	4.4	78	B2V			6
W259	18 18 40.965	-13 45 29.65	11.61	0.72	210	30000	4.4	148	B0V		_/B0.5V	14
W267	18 18 41.692	-13 46 43.86	13.13	0.52	125	14400	3.7	218	B5IV	bin[1]	_/B3V	0
W269	18 18 41.586	-13 42 48.02	13.98	0.93	55	22000	4.5	198	B2V			-4
W273	18 18 42.251	-13 47 30.42	14.21	0.71	85	9900	3.8	245	A0IV			-13
W275	18 18 42.250	-13 46 52.10	12.12	0.46	100	21900	4.5	75	B1V	bin[1]		8
W276	18 18 42.480	-13 48 47.02	13.74	0.67	100	13600	4.2	210	B6V			-2
W281	18 18 42.950	-13 46 42.80	13.80	0.59	30	8700	2.4	85	A3III-II			-1
W289	18 18 44.087	-13 48 56.49	12.60	0.50	170	18700	4.3	161	B2V		_/B3V	9
W292	18 18 43.683	-13 42 21.40	14.09	0.78	30	10500	4.1	86	B9V			6
W299	18 18 45.071	-13 49 19.42	14.46	0.69	30	8000	4.4	126	A6V	bin[1]		-16
W300	18 18 45.039	-13 47 47.17	12.69	0.52	145	18800	4.3	262	B2V			6
W305	18 18 44.970	-13 45 25.08	13.51	1.07	80	27000	4.4	205	B1V			7
W306	18 18 45.030	-13 45 41.02	12.77	0.68	100	21700	4.3	245	B1V			2
W307	18 18 45.320	-13 47 20.60	14.18	0.97	25	18700	4.1	135	B2V			2
W313	18 18 46.132	-13 49 23.43	12.92	0.50	140	13800	3.9	307	B6V	bin[1,3]	_/B5III	3
W323	18 18 46.743	-13 47 48.68	13.48	0.57	100	13800	4.1	257	B4V			4
W336	18 18 49.168	-13 48 04.23	13.29	0.52	110	13500	3.7	154	B5IV		_/B5III	7
W343	18 18 49.373	-13 46 50.05	11.72	0.85	155	_	_	_	_	SB2, bin[1]		28
W344	18 18 50.309	-13 54 24.32	13.63	0.87	10	<8000			<A8			-9
W347	18 18 49.363	-13 39 08.33	14.38	0.88	10	8000	3.3	38	A7III			-14
W351	18 18 50.683	-13 48 12.72	11.26	0.45	340	26400	4.3	232	B1V		_/B1V	2
W364	18 18 52.098	-13 49 29.20	13.44	0.53	100	11500	4.0	105	B7V	bin[1]		5
W368	18 18 53.372	-13 56 03.23	13.62	0.61	30	8000	2.5	144	A7III-II			-16
W371	18 18 53.012	-13 46 45.07	13.44	0.65	120	16500	4.3	213	B4V			12
W388	18 18 55.010	-13 48 46.10	13.70	0.58	35	13900	4.0	140	B7V			10
W389	18 18 55.590	-13 54 44.25	14.34	0.51	60	8500	3.8	213	A5IV			9
W400	18 18 55.832	-13 46 54.05	12.87	0.60	100	11400	3.8	44	B8IV	bin[1,2]	_/B9III	7
W409	18 18 57.369	-13 52 12.21	12.84	0.40	140	17200	4.3	192	B3V	bin[3]?	_/B2.5V	9
W444	18 19 00.428	-13 42 41.02	12.74	0.81	100	22000	4.3	110	B1V	bin[3]?	_/B1.5V	-10
W445	18 19 01.977	-13 53 28.29	14.16	0.48	80	9400	4.3	169	A1V			-6
W455	18 19 02.889	-13 47 17.67	12.11	0.60	15	8000	3.3	36	A6III		_/A5II	-16
W469	18 19 04.877	-13 48 20.44	10.69	0.40						bin[2] no L2	_/B0.5Vn	
W472	18 19 04.712	-13 44 44.54	12.97	0.50	80	13000	3.2	121	B6III	bin[2]	_/B3V+?	3
W473	18 19 05.706	-13 53 33.58	12.57	0.30	110	10000	2.9	266	A0III-II	bin[3]?	_/A0II	-33
W484	18 19 06.903	-13 45 04.50	12.46	0.46	80	12500	4.1	110	B7V		_/B8III	-13
W490	18 19 07.991	-13 46 00.71	13.07	0.44	130	10500	3.7	300	B9IV			-9
W495	18 19 08.953	-13 45 35.58	14.32	0.54	30	8500	4.4	103	A3V			-3
W496	18 19 09.653	-13 51 27.43	14.06	0.63	25	8500	3.7	102	A3IV			-19
W504	18 19 10.300	-13 49 03.85	12.78	0.42	145	12000	3.9	49	B8V		_/B9III	8
W515	18 19 13.040	-13 46 51.37	13.40	0.77	12	8000	4.5	10	A7V			20
W519	18 19 13.643	-13 49 20.19	13.71	0.72	37	8500	2.8	153	A3III-II			-3
W520	18 19 13.984	-13 52 21.71	11.64	0.46	186	13300	3.5	296	B5IV		_/B5IIIn	-14
W536	18 19 18.481	-13 55 40.09	11.46	0.22	196	21500	4.2	26	B2V	bin[2]	_/B1.5V +?	27
W541	18 19 19.127	-13 43 52.35	13.31	0.60	76	19000	4.2	59	B2V		_/B1-3V	10
W550	18 19 25.759	-13 46 39.13	13.66	0.68	21	8000	4.5	129	A8V			-23
W567	18 18 16.804	-13 58 46.45	11.99	0.36	82	18000	4.2	345	B2V			6
W568	18 18 20.474	-13 57 25.94	13.57	0.72	10	<8000			<A8			22
W570	18 18 15.094	-13 56 03.84	12.74	0.71	14	<8000			<A8			28

Table .2. continued.

Star	α	δ	V	B-V	S/N	$T_{\rm eff}$	log g	$V \sin i$	CFP	obs	lit.	RV
W582	18 18 20.234	-13 56 08.14	12.33	0.59	40	8400	3.4	90	A3IV	bin?		17
W587	18 18 56.667	-13 59 48.79	11.97	0.41	179	18300	4.3	131	B2V			1
W588	18 19 03.960	-14 00 00.20	12.18	0.38	21	8400	4.0	222	A3IV			29
W590	18 18 50.389	-13 57 04.36	12.29	0.31	50	10200	3.5	43	B8IV			25
W591	18 19 03.213	-13 56 07.39	11.74	0.40	146	13900	3.9	92	B5V			0
W596	18 19 25.295	-13 58 14.97	13.03	0.68	15	<8000			<A8			-18
W597	18 19 13.106	-13 57 38.28	12.30	0.39	124	17800	4.3	237	B2V			6
W607	18 19 32.824	-13 55 50.67	12.48	0.47	65	16000	4.3	69	B3V			8
W625	18 18 08.154	-13 53 16.63	14.07	0.55	37	10500	4.0	254	A0V			12
W626	18 18 09.471	-13 55 40.36	13.92	0.76	9	<8000			<A8			29
W627	18 18 14.285	-13 57 57.03	13.97	0.49	22	10000	4.5	181	A0V			-5
W632	18 19 13.569	-13 57 13.85	14.36	0.54	39	9000	3.9	55	A2V			-7
W633	18 19 16.670	-13 57 31.50	13.76	0.66	8	<8000			<A8			28:
W639	18 19 26.230	-13 47 25.50	13.08	0.61	13	8000	4.3	5	A6V			28:
WFI[N6611]017	18 19 17.083	-13 54 50.64	14.29	0.64	55	9600	4.2	169	A1V	Bew **ELS**		22
W031	18 18 10.121	-13 50 41.15	14.40	0.40	50	9000	3.7	156	A2IV	**ELS**		33
W080	18 18 18.201	-13 41 59.25	13.82	1.64	35	24000	4.3	183	B1V	**ELS**	B2V/_	3
W235	18 18 38.817	-13 46 44.28	10.98	0.82	170	24000:	3.5:	482:	B1IV	**HBe**	HBe/HBe	12
W301	18 18 44.980	-13 46 24.90	12.22	0.57	210	20600	4.2	115	B2V	**ELS**	_/B2V	5
W483	18 19 06.506	-13 43 30.47	10.99	0.41	195	14600	3.6	186	B3IV	Bew **ELS**	_/B3V	-13
W500	18 19 09.019	-13 43 14.95	11.28	0.43	190	13700	3.4	289	B5IV	Bew **ELS**	_/B5e	-16
W503	18 19 11.068	-13 56 43.08	9.75	0.49	90	23500:	3.0:	236:	B1III	Bew[3] **ELS**	_/B1:e	-9
W601	18 19 20.031	-13 54 21.67	10.68	0.36		22500[4]	4.0[4]	190[4]		no L2,**ELS**	B1.5V/_	

bin[1] the star was detected as a binary by Duchêne et al. (2001)
bin[2] the difference in RV between this paper and Evans et al. (2005) is larger than 15km s^{-1}
bin[3] the difference in RV between this paper and Evans et al. (2005) is between 10 and 15km s^{-1}
[4] fundamental parameters from Alecian et al. (2008).

Table .3. Associated parameters for stars: mass (col. 2), luminosity (col. 3), radius (col. 4), and age in Myears (col. 5). The corresponding errors are: ±0.5 to 1.5 in $M/M_{\odot}$, ±0.3 in $\log(L/L_{\odot})$, ±0.5 to 1.5 in $R/R_{\odot}$, and ±1 to 25 Myears for the age, depending on the value of the parameter and the initial S/N ratio of spectrum.

Star	$M/M_{\odot}$	$\log(L/L_{\odot})$	$R/R_{\odot}$	Age (Myears)
WFI014a	8.9	4.05	24.9	27
WFI019	7.8	3.84	23.5	37
WFI125	8.9	4.05	56.5	27
WFI152	2.3	1.62	3.2	646
W002	-	-	-	-
W018	1.7	0.93	1.5	33
W024	2.4	1.77	4.0	717
W025	9.4	3.67	3.8	1
W026	2.7	1.91	3.8	448
W035	2.3	1.44	1.8	28
W036	1.8	1.04	1.8	510
W041	-	-	-	-
W064	6.5	3.51	30.4	55
W090	4.3	2.60	3.1	62
W125	-	-	-	-
W161	23.0	4.92	7.9	3
W166	-	-	-	-
W175	-	-	-	-
W188	15.7	4.36	5.2	0.5
W194	-	-	-	-
W201	6.2	3.47	18.7	64
W202	3.4	2.20	2.7	122
W203	2.4	1.71	2.9	473
W223	9.8	3.73	3.9	0.9
W228	7.4	3.33	3.4	1.4
W231	9.6	3.70	3.9	1
W238	2.5	1.81	3.3	459
W239	6.8	3.20	3.2	2.5
W243	4.4	2.51	2.5	4.9
W251	6.8	3.20	3.2	2.5
W259	14.1	4.22	4.8	0.5
W267	5.0	3.02	5.3	82
W269	7.7	3.39	3.4	1.2
W273	2.9	2.02	3.5	333
W275	7.7	3.38	3.4	1.3
W276	3.7	2.28	2.5	53
W281	6.7	3.56	27	52
W289	5.9	2.99	3.0	5.5
W292	2.7	1.79	2.4	232
W299	1.7	0.93	1.5	33
W300	6.0	3.00	3.0	5.3
W305	11.3	3.92	4.2	0.4
W306	7.5	3.35	3.4	1.3
W307	6.3	3.16	3.7	25
W313	4.3	2.67	3.8	104
W323	3.9	2.43	2.9	81
W336	4.6	2.87	5.0	106
W343	-	-	-	-
W344	-	-	-	-
W347	2.8	2.14	6.2	442
W351	10.8	3.86	4.1	0.6
W364	3.2	2.12	2.9	193
W368	5.5	3.23	22.0	83
W371	4.7	2.65	2.6	3
W388	4.1	2.57	3.4	94
W389	2.4	1.68	3.2	587
W400	3.5	2.35	3.9	211
W409	5.1	2.78	2.8	8
W444	7.7	3.39	3.4	1.2
W445	2.1	1.30	1.7	37
W455	2.8	2.14	6.2	442
W469	-	-	-	-
W472	5.8	3.40	10.1	73
W473	5.1	3.19	13.4	92
W484	3.4	2.20	2.7	122
W490	3.3	2.28	4.2	259
W495	1.9	1.07	1.6	38
W496	2.5	1.80	3.7	512
W504	3.5	2.35	3.5	180
W515	1.7	0.93	1.5	33
W519	4.5	2.96	14.2	128
W520	4.8	3.06	6.6	110
W536	7.6	3.39	3.6	6
W541	6.2	3.09	3.3	12
W550	1.7	0.93	1.5	33
W567	5.7	2.95	3.1	16
W568	-	-	-	-
W570	-	-	-	-
W582	2.8	2.12	5.5	457
W587	5.7	2.94	3.0	6
W588	2.1	1.40	2.4	637
W590	3.4	2.44	5.4	286
W591	4.3	2.69	3.9	102
W596	-	-	-	-
W597	5.4	2.87	2.9	7
W607	4.5	2.57	2.6	4.1
W625	2.8	1.91	2.8	271
W626	-	-	-	-
W627	2.3	1.44	1.8	28
W632	2.4	1.68	2.9	498
W633	-	-	-	-
W639	1.7	0.93	1.5	33

Table .3. continued.

Star	$M/M_{\odot}$	$\log(L/L_{\odot})$	$R/R_{\odot}$	Age (Myears)
WFI017	2.3	1.47	2.0	239
W031	2.7	1.93	3.8	432
W080	8.9	3.61	3.7	0.5
W235	13.9:	4.55:	11:	12:
W301	7.0	3.28	3.5	7
W483	5.4	3.17	6.1	79
W500	5.4	3.26	7.8	85
W503	21.7:	5.20:	24.9:	7:
W601	-	-	-	-

Table .4. Equivalent widths of interstellar absorption bands at 4430Å (col. 2) and at 6613 Å (col. 3) and their corresponding E[B-V] (cols. 4 and 5) from the calibration of Herbig (1975). The mean E(B-V) is given in col. 6. In cols. 7, 8 and 9 the J, H and K magnitudes from 2MASS are given. In cols. 10 and 11 the $(J-H)_0$ and $(H-K)_0$ colours obtained with the mean E(B-V) and 2MASS magnitudes are given. In cols. 12, 13, 14, and 15 the magnitudes at 3.6, 4.5, 5.8 and 8 μm from SPITZER are given (archive, release Spring07). In cols. 16 and 17 the $(3.6\text{-}4.5)_0$ and $(5.8\text{-}8)_0$ colours obtained with the mean E(B-V) and SPITZER magnitudes are given. The corresponding errors are: ±0.0010 to 0.0020 for the EW and ±0.005 in the E[B-V]. The mean errors on the 2MASS magnitudes and 2MASS colour indexes are ±0.060, while for SPITZER magnitudes the mean error is ± 0.045. Note that for the calculations one more digit was kept.

Star Star	EW 4430	EW 6613	E(B-V) 4430	E(B-V) 6613	<E(B-V)>	J	H	K	$(J-H)_0$	$(H-K)_0$	3.6	4.5	5.8	8.0	$(3.6\text{-}4.5)_0$	$(5.8\text{-}8)_0$
WFI014a	_	0.016	_	0.638	0.638	12.986	12.713	12.573	0.061	0.015	12.517	12.463	_	_	_	_
WFI019	_	0.015	_	0.622	0.622	12.966	12.656	12.598	0.104	-0.063	12.527	12.470	11.939	_	_	_
WFI125	_	0.013	_	0.541	0.541	12.520	12.158	11.920	0.183	0.132	11.902	_	_	_	_	_
WFI152	0.134	0.021	0.589	0.837	0.713	11.946	11.722	11.558	-0.013	0.025	11.478	11.398	11.148	_	_	_
W002	_	0.014	_	0.557	0.557	9.643	9.538	9.472	-0.080	-0.043	9.439	9.441	9.452	9.361	-0.062	0.086
W018	0.091	0.017	0.400	0.703	0.552	12.704	12.405	12.106	0.116	0.191	12.259	12.086	_	_	_	_
W024	_	0.021	_	0.842	0.841	12.500	12.235	12.141	-0.014	-0.070	12.071	12.019	11.875	_	_	_
W025	0.307	0.022	1.352	0.886	1.119	10.195	9.766	9.490	0.058	0.057	9.485	9.451	9.452	9.390	-0.087	0.052
W026	0.256	0.020	1.128	0.801	0.965	11.996	11.664	11.047	0.012	0.429	11.614	11.493	11.696	11.234	0.016	0.453
W035	0.149	0.023	0.656	0.919	0.787	12.796	12.350	12.348	0.185	-0.152	12.003	12.047	12.200	_	_	_
W036	0.125	0.015	0.550	0.594	0.572	11.877	11.672	11.555	0.015	0.005	11.558	11.340	11.126	_	_	_
W041	0.185	0.015	0.816	0.594	0.705	12.270	11.951	11.805	0.085	0.008	11.699	11.734	11.564	_	_	_
W064	0.111	0.014	0.488	0.557	0.522	11.997	11.774	11.631	0.050	0.041	11.484	11.380	11.453	11.398	0.047	0.050
W090	0.141	0.017	0.622	0.695	0.659	10.808	10.706	10.599	-0.117	-0.022	10.609	10.589	10.614	10.566	-0.052	0.042
W125	_	0.021	_	0.862	0.862	8.823	8.692	8.596	-0.155	-0.072	8.568	8.590	8.512	8.573	-0.116	-0.069
W161	0.280	0.029	1.236	1.183	1.209	8.156	7.732	7.453	0.023	0.043	7.323	7.219	7.187	7.246	-0.027	-0.070
W166	_	0.029	_	1.175	1.175	8.876	8.736	8.596	-0.250	-0.089	8.588	8.588	8.528	8.506	-0.127	0.011
W175	_	0.022	_	0.898	0.898	7.590	7.223	7.006	0.069	0.042	7.149	6.907	6.799	6.858	0.145	-0.067
W188	0.408	0.041	1.800	1.675	1.737	9.534	9.074	8.776	-0.116	-0.041	8.624	8.631	8.561	8.571	-0.195	-0.026
W194	0.070	0.023	0.309	0.927	0.618	12.400	11.909	12.013	0.286	-0.225	11.930	11.922	11.716	_	_	_
W201	_	0.016	_	0.646	0.646	11.948	11.681	11.571	0.053	-0.016	11.478	11.567	11.644	_	_	_
W202	0.215	0.022	0.948	0.882	0.915	11.821	11.440	11.231	0.077	0.030	11.057	11.006	11.034	_	_	_
W203	0.090	0.019	0.397	0.756	0.576	_	_	_	_	_	12.258	12.215	11.828	_	_	_
W223	0.279	0.021	1.230	0.862	1.046	9.543	9.306	9.193	-0.110	-0.091	9.099	9.141	9.069	9.223	-0.155	-0.164
W228	0.279	0.026	1.230	1.045	1.137	10.789	10.384	10.082	0.028	0.080	10.221	_	9.842	_	_	_
W231	0.266	0.023	1.172	0.947	1.060	10.590	10.213	10.057	0.025	-0.051	9.946	9.940	9.908	9.950	-0.109	-0.052
W238	0.130	0.020	0.573	0.797	0.685	11.539	11.274	11.078	0.038	0.062	10.941	10.803	10.883	10.732	0.064	0.145
W239	0.182	0.019	0.802	0.756	0.779	10.396	10.274	10.164	-0.136	-0.042	10.087	10.072	9.899	9.294	-0.070	0.598
W243	0.209	0.024	0.921	0.980	0.950	11.985	11.632	11.395	0.038	0.051	11.107	11.108	11.221	11.335	-0.104	-0.123
W251	0.211	0.022	0.930	0.878	0.904	11.399	11.044	10.884	0.055	-0.017	10.785	10.839	10.715	_	_	_
W259	0.254	0.023	1.119	0.919	1.019	9.614	9.315	9.193	-0.039	-0.077	9.104	9.124	9.033	9.152	-0.131	-0.128
W267	0.171	0.021	0.754	0.837	0.796	11.653	11.462	11.366	-0.073	-0.059	11.237	11.237	11.190	11.360	-0.086	-0.177
W269	0.288	0.026	1.269	1.069	1.169	11.303	10.854	10.647	0.061	-0.021	10.432	10.366	10.255	_	_	_
W273	0.194	0.023	0.855	0.947	0.901	12.256	11.901	11.624	0.056	0.101	11.615	11.554	11.222	_	_	_
W275	0.207	0.020	0.912	0.801	0.857	10.810	10.651	10.530	-0.125	-0.046	10.530	10.447	10.631	10.769	-0.010	-0.146
W276	0.163	0.021	0.718	0.862	0.790	11.973	11.573	11.392	0.138	0.027	11.307	11.277	11.204	11.075	-0.056	0.122

Table .4. continued

W281	0.150	0.023	0.661	0.927	0.794	12.087	11.928	11.773	-0.104	0.000	11.796	11.747	11.778	_	_	_
W289	0.182	0.021	0.802	0.850	0.826	11.186	10.996	10.895	-0.084	-0.060	10.611	10.732	10.650	10.476	-0.211	0.166
W292	0.167	0.018	0.736	0.732	0.734	12.483	12.280	12.137	-0.040	0.000	12.036	12.047	11.642	_	_	_
W299	0.146	0.020	0.644	0.801	0.722	12.445	12.080	11.664	0.126	0.275	12.040	12.117	_	_	-0.155	_
W300	0.200	0.021	0.881	0.842	0.861	11.185	10.973	10.582	-0.074	0.223	10.845	10.822	10.685	_	_	_
W305	0.312	0.023	1.375	0.943	1.159	10.488	10.050	9.795	0.054	0.029	9.641	9.638	9.598	_	_	_
W306	0.186	0.021	0.820	0.862	0.841	10.863	10.593	10.539	-0.009	-0.110	10.435	10.485	10.537	_	_	_
W307	0.216	0.027	0.952	1.081	1.017	11.733	11.314	10.341	0.082	0.774	10.954	10.762	_	_	_	_
W313	0.168	0.019	0.740	0.789	0.765	11.594	11.383	11.247	-0.043	-0.013	11.140	11.104	10.910	10.709	-0.047	0.194
W323	0.182	0.022	0.802	0.886	0.844	11.906	11.655	11.534	-0.029	-0.044	11.447	11.462	11.683	_	_	_
W336	0.185	0.020	0.815	0.825	0.820	11.804	11.612	11.455	-0.080	-0.003	11.391	11.232	10.900	_	_	_
W343	0.267	0.022	1.177	0.911	1.044	9.476	9.119	8.900	0.011	0.015	8.742	8.744	8.669	8.831	-0.115	-0.172
W344	_	0.014	_	0.581	0.581	11.907	11.527	11.382	0.187	0.032	_	11.266	_	_	_	_
W347	0.184	0.024	0.809	0.972	0.890	12.512	12.199	12.077	0.018	-0.052	11.949	12.015	11.625	_	_	_
W351	0.254	0.020	1.119	0.809	0.964	9.994	9.783	9.670	-0.109	-0.075	9.667	9.608	9.578	9.368	-0.046	0.201
W364	0.164	0.019	0.723	0.768	0.746	11.734	11.418	11.131	0.069	0.141	10.717	10.948	10.476	_	_	_
W368	0.125	0.014	0.551	0.553	0.552	12.091	11.875	11.694	0.033	0.073	11.704	11.735	11.790	_	_	_
W371	0.175	0.021	0.771	0.833	0.802	11.671	11.398	11.163	0.007	0.078	10.907	10.845	10.829	_	_	_
W388	0.165	0.026	0.727	1.053	0.890	12.186	11.973	11.812	-0.082	-0.013	11.621	11.518	11.271	_	_	_
W389	0.070	0.015	0.309	0.626	0.467	12.982	12.812	12.631	0.015	0.090	12.439	_	_	_	_	_
W400	0.182	0.018	0.802	0.732	0.767	11.001	10.689	10.394	0.058	0.145	10.166	10.018	9.825	9.378	0.065	0.440
W409	0.152	0.015	0.670	0.622	0.646	11.585	11.403	9.908	-0.032	1.369	11.405	11.254	_	_	0.081	_
W444	0.221	0.021	0.974	0.854	0.914	10.300	9.958	9.744	0.039	0.035	9.647	9.668	9.458	9.088	-0.120	0.361
W445	0.084	0.017	0.370	0.675	0.523	12.840	12.728	12.596	-0.061	0.030	12.744	12.690	_	_	-0.003	_
W455	_	0.022	_	0.882	0.882	10.815	10.667	10.540	-0.145	-0.045	10.528	10.518	10.348	10.252	-0.086	0.088
W469	_	0.020	_	0.817	0.817	9.576	9.449	9.310	-0.144	-0.021	9.283	9.122	8.740	_	_	_
W472	0.177	0.020	0.780	0.829	0.805	11.610	11.507	11.397	-0.164	-0.047	11.441	11.366	11.406	_	_	_
W473	0.140	0.017	0.617	0.703	0.660	11.508	11.416	11.333	-0.127	-0.046	11.272	11.243	10.913	10.160	-0.043	0.747
W484	0.182	0.018	0.802	0.740	0.771	11.237	11.144	11.052	-0.163	-0.059	10.982	11.008	11.000	_	_	_
W490	0.151	0.019	0.666	0.785	0.725	11.896	11.798	11.733	-0.142	-0.077	11.707	11.626	11.221	_	_	_
W495	0.115	0.019	0.507	0.781	0.644	12.734	12.746	12.555	-0.226	0.065	12.667	12.521	_	_	0.076	_
W496	0.113	0.020	0.498	0.805	0.651	12.523	12.346	12.173	-0.039	0.046	12.074	12.103	_	_	-0.100	_
W504	0.147	0.020	0.648	0.821	0.735	11.677	11.603	11.510	-0.170	-0.051	11.504	11.443	11.206	_	_	_
W515	0.150	0.018	0.661	0.732	0.696	11.496	11.181	11.036	0.084	0.009	11.036	10.955	11.021	_	_	_
W519	0.094	0.019	0.414	0.756	0.585	12.083	11.772	11.653	0.117	0.005	11.588	11.525	11.647	_	_	_
W520	0.162	0.020	0.713	0.825	0.769	10.498	10.358	10.264	-0.115	-0.056	10.231	10.144	10.054	9.744	0.004	0.303
W536	0.200	0.018	0.881	0.732	0.807	10.471	10.357	10.260	-0.154	-0.061	10.248	10.234	10.130	9.639	-0.074	0.483
W541	0.216	0.020	0.952	0.797	0.874	11.579	11.351	11.194	-0.062	-0.014	11.181	11.183	11.095	11.032	-0.097	0.055
W550	0.174	0.019	0.767	0.781	0.774	12.135	11.931	11.789	-0.053	-0.009	11.782	11.754	11.340	_	_	_

Table .4. continued

W567	0.168	0.018	0.740	0.732	0.736	11.047	10.943	10.839	-0.140	-0.040	10.886	10.955	10.796	10.912	-0.149	-0.123
W568	_	0.014	_	0.577	0.577	12.015	11.757	11.387	0.067	0.257	11.543	11.459	11.272	_	0.021	_
W570	_	0.015	_	0.606	0.606	11.164	10.893	10.814	0.070	-0.039	10.810	10.778	10.629	10.674	-0.034	-0.051
W582	_	0.014	_	0.549	0.549	10.837	10.490	10.334	0.165	0.049	10.369	10.314	10.334	10.210	-0.005	0.119
W587	0.149	0.017	0.657	0.675	0.666	10.909	10.834	10.763	-0.146	-0.059	10.729	10.855	10.849	_	-0.198	_
W588	0.170	0.012	0.749	0.480	0.614	11.321	11.160	11.028	-0.043	0.012	11.030	11.159	10.812	10.958	-0.196	-0.152
W590	0.070	0.014	0.309	0.565	0.437	11.396	11.261	11.190	-0.010	-0.014	11.148	11.168	11.444	_	-0.067	_
W591	0.146	0.017	0.644	0.703	0.673	10.679	10.599	10.494	-0.143	-0.026	10.489	10.451	10.550	_	-0.035	_
W596	_	0.012	_	0.480	0.480	11.505	11.233	10.723	0.113	0.416	10.985	11.087	11.076	_	-0.154	_
W597	0.179	0.018	0.789	0.740	0.764	11.241	11.134	11.071	-0.146	-0.086	11.012	11.056	11.032	_	-0.127	_
W607	0.140	0.016	0.617	0.646	0.632	11.158	10.865	10.713	0.083	0.029	10.644	10.656	10.516	10.669	-0.081	-0.159
W625	0.112	0.023	0.494	0.947	0.720	12.489	12.223	12.119	0.027	-0.037	12.084	11.977	11.987	_	_	_
W626	_	0.017	_	0.699	0.699	12.045	11.656	11.544	0.157	-0.025	11.409	11.446	11.498	_	_	_
W627	0.200	0.019	0.881	0.789	0.835	12.504	11.349	10.574	0.878	0.612	_	_	_	_	_	_
W632	0.080	0.018	0.353	0.740	0.546	12.816	12.620	12.480	0.015	0.033	12.366	12.393	_	_	-0.086	_
W633	_	0.016	_	0.650	0.650	12.049	11.712	10.695	0.121	0.890	11.541	11.520	11.339	11.785	-0.050	-0.452
W639	0.130	0.017	0.573	0.699	0.636	11.637	11.440	11.357	-0.014	-0.041	11.246	11.199	10.850	_	-0.022	_
WFI017	0.172	0.018	0.757	0.728	0.742	12.581	11.882	11.083	0.453	0.654	9.708	9.108	8.455	7.022	0.519	1.426
W031	0.177	0.025	0.781	1.016	0.898	12.729	12.502	12.420	-0.071	-0.093	12.438	12.279	12.069	11.5*	0.062	0.561*
W080	0.552	0.032	2.432	1.301	1.866	10.103	9.596	9.304	-0.112	-0.072	9.062	9.015	8.936	8.900	-0.155	0.019
W235	0.240	0.022	1.058	0.898	0.978	8.563	8.121	7.714	0.118	0.216	7.180	6.844	6.525	6.226	0.230	0.290
W301	0.217	0.021	0.956	0.854	0.905	10.631	10.402	10.304	-0.071	-0.079	10.248	10.244	10.145	10.390	-0.094	-0.253
W483	0.172	0.018	0.758	0.736	0.747	9.875	9.762	9.608	-0.135	0.008	9.453	9.293	9.146	8.956	0.079	0.183
W500	0.151	0.017	0.666	0.703	0.684	10.055	9.904	9.785	-0.076	-0.015	9.646	9.447	9.332	9.072	0.125	0.254
W503	0.232	0.017	_	0.687	0.687	8.726	8.430	8.105	0.034	0.171	7.044	6.794	6.594	6.305	0.164	0.282
W601	_	0.017	_	0.691	0.691	9.703	9.523	9.398	-0.049	-0.010	9.298	9.285	9.261	9.134	-0.062	0.121
W245	_	_	_	_	0.791	11.199	10.475	9.776	0.462	0.545	8.425	7.823	7.482	7.073	0.516	0.402
W494	_	_	_	_	0.791	11.770	10.690	9.543	0.818	0.993	7.736	7.146	6.428	5.465	0.504	0.956

* As the magnitude is not present, we give to the star the limiting magnitude of the archive.

Table .5. Indications for each star about its nature: in col. 2, about the binarity, in col. 3 from IR data of 2MASS (Y:med is for a mediul infrared excess, Y: strong for a strong infrared excess), in col. 4 from IR data of SPITZER (class I, class II, MS for Main Sequence, Y:med is for a medium infrared excess without obvious classification in classI/II or MS), in col. 5, the age interpolated from MS HR diagrams, in col. 6, according to MS age interpolated too old for this region. In col. 7, indications on the nature of the stars from previous studies (Walker 1961; Belikov et al. 1999; Hillenbrand et al. 1993; Herbig & Dahm 2001; Evans et al. 2005; Indebetouw et al. 2007) are given. In col. 8, the mass of the star is provided. In col. 9 and 10, the membership probabilities from Tucholke et al. (1986,Tu86) and from Belikov et al. (1999,Bel99) are given. In col. 11, the deduced status (PMS or MS) for each star in function of previous information is given. In col. 12, the age interpolated from PMS tracks, is given, and in the last column, the age (in Myears) finally selected for each star in function of its nature is provided. The error in this age ranges from 0.02 to 25 Myear depending on the value of the age. '_' stands for no available information or data.

Star	Bin?	2MASS	class	age MS	old	other	mass	Tu86	Bel99	new status	age PMS	age kept
WFI014a	N	N	_	27	no		8.9	_	_	MS?	0.04	27
WFI019	N	N	_	37	no		7.8	_	0	MS	0.03	37
WFI125	N	N	_	27	no		8.9	_	_	MS?	0.01	27
WFI152	N	N	_	646	yes		2.3	_	26	PMS?	2.2	2.2
W002	N	N	_	_	_		_	29	8	MS	_	_
W018	N	N	_	33	no		1.7	0	11	MS	8.6	33
W024	N	N	_	717	yes		2.4	_	5	PMS?	2	2
W025	yes	N	_	1	no		9.4	94	53	MS	_	1
W026	N	Y:med	Y:med	448	yes		2.7	78	62	PMS	1	1
W035	N	N	_	28	no		2.3	90	51	PMS?	_	28>
W036	N	N	_	510	yes	PMS[1]	1.8	71	49	PMS?	0.9	0.9
W041	N	N	_	_	_		_	0	42	MS	_	_
W064	N	N	_	55	yes		6.5	0	11	MS	0.02	55
W090	N	N	_	62	yes		4.3	93	77	PMS	1	1
W125	yes	N	MS	_	_		_	94	79	MS	_	_
W161	yes	N	MS	3	no	MS[2]	23	94	70	MS	_	3
W166	N	N	MS	_	_		_	94	95	MS	_	_
W175	yes	N	MS	_	_	MS[2]	_	94	95	MS	_	_
W188	yes	N	MS	0.5	no	MS[2]	15.7	87	68	MS	_	0.5
W194	N	N	_	_	_		_	73	67	MS	_	_
W201	N	N	_	64	yes		6.2	0	5	MS?	0.03	64?
W202	N	N	_	122	yes	PMS[2]	3.4	0	0	PMS	1.1	1.1
W203	N	_	_	473	yes		2.4	93	90	PMS	2.3	2.3
W223	N	N	MS	0.9	no		9.8	94	89	MS	_	0.9
W228	N	N	_	1.4	no		7.4	91	86	MS	_	1.4
W231	N	N	MS	0.9	no		9.6	93	78	MS	_	0.9
W238	N	N	_	459	yes		2.5	94	56	PMS	0.9	0.9
W239	yes	N	Y:med	2.5	no		6.8	94	67	MS	_	2.5
W243	yes	N	MS	4.9	no		4.4	93	93	MS	_	4.9
W251	N	N	_	2.5	no		6.8	0	_	MS	_	2.5
W259	N	N	MS	0.5	no		14.1	94	87	MS	_	0.5
W267	yes	N	MS	82	yes	PMS[2]	5	92	87	PMS	0.3	0.3
W269	N	N	_	1.2	no		7.7	_	26	MS	_	1.2
W273	N	N	_	333	yes	PMS[2]	2.9	94	58	PMS	0.9	0.9
W275	yes	N	MS	1.3	no		7.7	0	0	MS	_	1.3
W276	N	N	_	53	yes?	PMS[2]	3.7	89	69	PMS	1	1
W281	N	N	_	52	yes		6.7	94	96	PMS	0.02	0.02
W289	N	N	_	5.5	no		5.9	91	95	MS?	_	5.5
W292	N	N	_	232	yes		2.7	29	81	PMS	2	2
W299	yes	Y:med	_	33	no	PMS[2]	1.7	0	55	PMS	10	10
W300	N	N	_	5.3	no		6	_	16	MS	_	5.3
W305	N	N	_	0.4	no		11.3	92	84	MS	_	0.4
W306	N	N	_	1.3	no		7.5	89	96	MS	0.4	1.3
W307	N	Y:strong	_	25	no		6.3	_	76	PMS	0.03	0.03
W313	yes	N	_	104	yes	PMS[2]	4.3	81	90	PMS	2	2
W323	N	N	_	81	yes		3.9	2	58	PMS?	1.1	1.1?
W336	N	N	_	106	yes		4.6	87	88	PMS	0.3	0.3
W343	yes	N	MS	_	_		_	93	83	MS	_	_
W344	N	N	_	_	_		_	0	0	MS?	_	_
W347	N	N	_	442	yes		2.8	_	66	PMS	0.6	0.6
W351	N	N	_	0.6	no		10.8	94	91	MS	_	0.6
W364	yes	N	_	193	yes?		3.2	93	_	PMS	1	1
W368	N	N	_	83	yes?		5.5	27	10	MS?	0.08	83?
W371	N	N	_	3	no		4.7	40	72	MS	_	3
W388	N	N	_	94	yes	PMS[2]	4.1	91	90	PMS	2	2
W389	N	N	_	587	yes		2.4	0	1	PMS?	2	2?
W400	yes	N	Y:med	211	yes	PMS[2]	3.5	93	82	PMS	1	1
W409	yes	Y:strong	_	8	no		5.1	94	66	PMS	_	_
W444	yes	N	Y:med	1.2	no		7.7	0	70	PMS	_	_
W445	N	N	_	37	no		2.1	22	58	PMS?	7	7
W455	N	N	_	442	yes	PMS[2]	2.8	7	7	PMS	0.3	0.3
W469	yes	N	_	_	_		_	94	70	MS	_	_
W472	yes	N	_	73	yes		5.8	91	12	PMS?	0.2	0.2?
W473	yes	N	Y:med	92	yes	accr disk[3]	5.1	92	48	PMS	0.1	0.1
W484	N	N	_	122	yes?		3.4	94	38	PMS?	1.2	1.2?
W490	N	N	_	259	yes		3.3	92	67	PMS	0.5	0.5
W495	N	N	_	38	yes?		1.9	90	56	PMS	6	6
W496	N	N	_	512	yes		2.5	27	34	PMS?	0.8	0.8?
W504	N	N	_	180	yes		3.5	92	25	PMS?	1	1?
W515	N	N	_	33	yes?		1.7	90	68	PMS	8	8
W519	N	N	_	128	yes		4.5	0	0	MS?	0.7	128?
W520	N	N	Y:med	110	yes		4.8	94	46	PMS	0.2	0.2
W536	yes	N	Y:med	6	no		7.6	94	39	PMS?	_	6>?
W541	N	N	_	12	yes?		6.2	92	56	MS?	0.2	12?
W550	N	N	_	33	yes?		1.7	91	38	PMS?	8	8?
W567	N	N	MS	16	no		5.7	5	17	MS	0.03	16
W568	N	Y:med	_	_	_		_	29	15	MS	_	_
W570	N	N	MS	_	_		_	0	5	MS	_	_
W582	yes	N	_	457	yes		2.8	0	7	PMS?	0.7	0.7?
W587	N	N	_	6	no		5.7	_	35	MS	_	6
W588	N	N	MS	637	yes		2.1	_	18	PMS?	2	2?

Table .5. continued.

Star	Bin?	2MASS	class	age MS	old	other	mass	Tu86	Bel99	new status	age PMS	age kept
W590	N	N	_	286	yes		3.4	92	34	PMS?	0.4	0.4?
W591	N	N	_	102	yes		4.3	82	11	PMS?	0.2	0.2?
W596	N	Y:strong	_	_	_		_	15	16	PMS	_	_
W597	N	N	_	7	no		5.4	94	38	MS	_	7
W607	N	N	MS	4	no		4.5	_	18	MS	_	4
W625	N	N	_	271	yes		2.8	88	57	PMS	0.9	0.9
W626	N	N	_	_	no		_	1	23	MS	_	_
W627	N	Y:strong	_	28	no		2.3	92	21	PMS?	2.8	2.8?
W632	N	N	_	498	yes		2.4	0	0	PMS?	1.6	1.6?
W633	N	Y:strong	MS	_	_		_	0	2	MS?	_	_
W639	N	N	_	33	no		1.7	93	15	MS?	8	33?
WFI017	N	Y:strong, HBe/Ae	class I	239	yes	accr disk[3]	2.3	_	1	PMS	3	3
W031	N	N	class II?	432	no?		2.7	1	21	PMS?	1	1
W080	N	N	MS	0.5	no		8.9	0	24	MS	_	0.5
W235	N	Y:med	Y:med	12:	yes		13.9:	94	96	PMS	0.02	0.02
W301	N	N	MS	7	no		7	94	92	MS	_	7
W483	N	N	Y:med	79	yes	PMS[4]	5.4	93	72	PMS	0.1	0.1
W500	N	N	Y:med	85	yes	PMS[4]	5.4	94	54	PMS	0.1	0.1
W503	yes	Y:med	Y:med	7:	yes		21.7:	94	40	MS?, bin	0.02	7?
W601	N	N	MS?	_	_	PMS[5]	10.2[5]	93	43	PMS?	0.016[5]	0.016[5]
W245	N	Y:strong, HBe/Ae	class II	_	_	PMS[2]	_	0	1	PMS	_	_
W494	N	Y:strong, HBe/Ae	class II	_	_	PMS[2]	_	1	_	PMS	_	_

[1] indication from Ogura et al. (2002)
[2] indication from Walker (1961)
[3] indication from Indebetouw et al. (2007)
[4] indication from Tucholke et al. (1986)
[5] indication from Alecian et al. (2008).

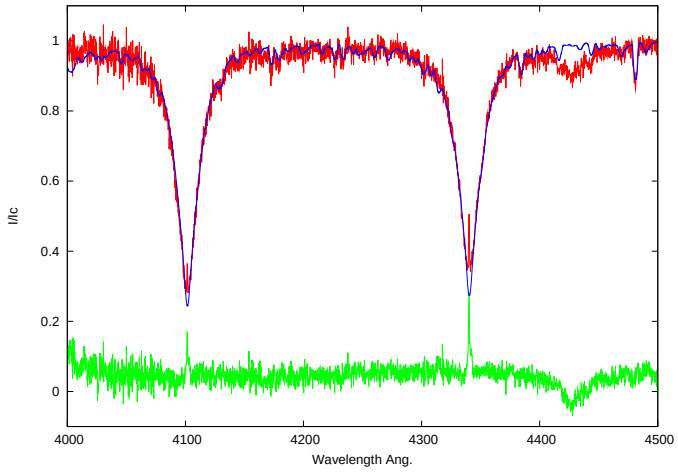

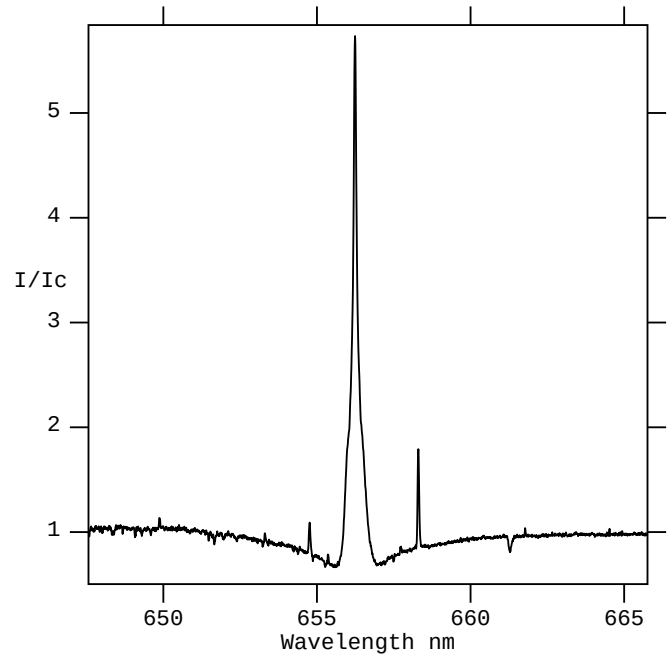

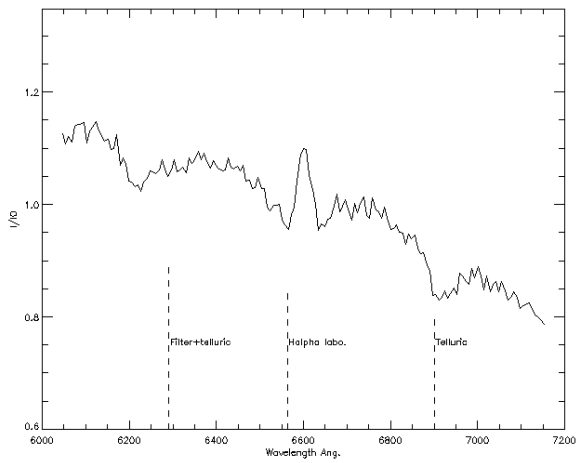

Fig. .10. ELS WFI017. Top panel: fit of the LR2 range of the spectrum for the fundamental parameters determination. The observed spectrum is in red, the fit in blue, the residuals in green; middle panel: Hα line from the VLT-GIRAFFE; bottom panel: Hα line from the WFI-spectro.

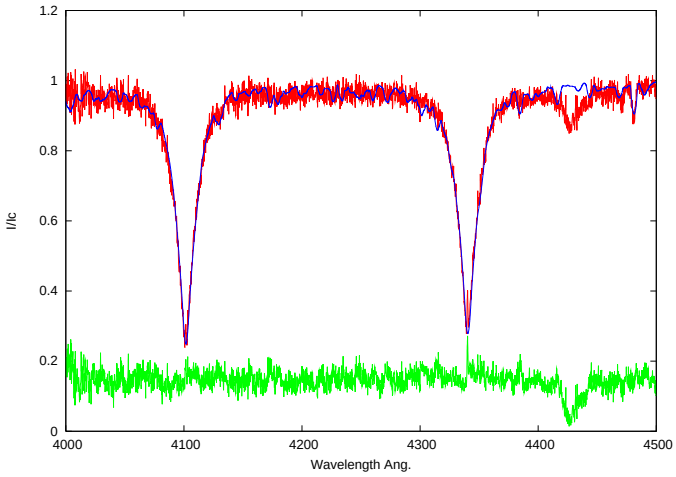

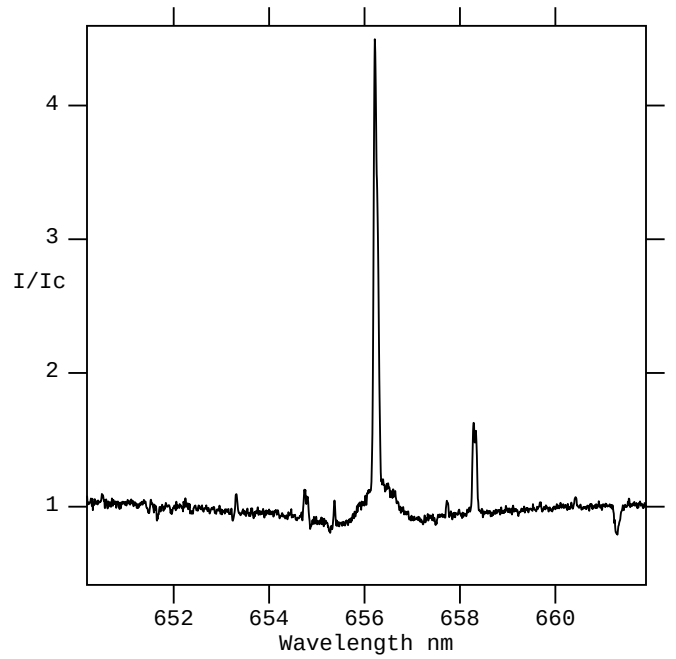

Fig. .11. ELS W031. Top panel: fit of the LR2 range of the spectrum for the fundamental parameters determination. The observed spectrum is in red, the fit in blue, the residuals in green; bottom panel: Hα line from the VLT-GIRAFFE.

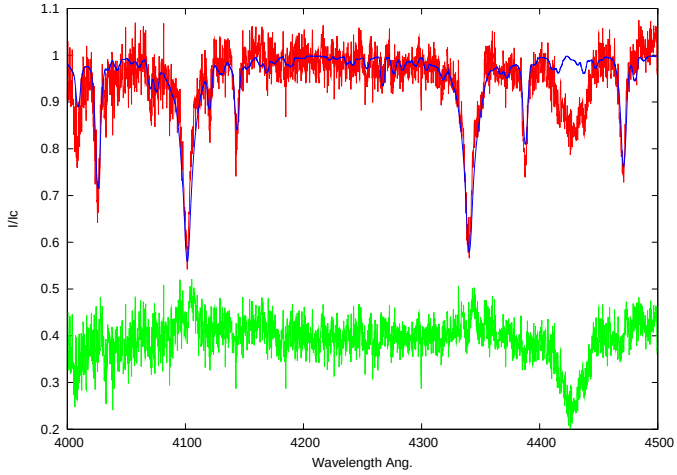

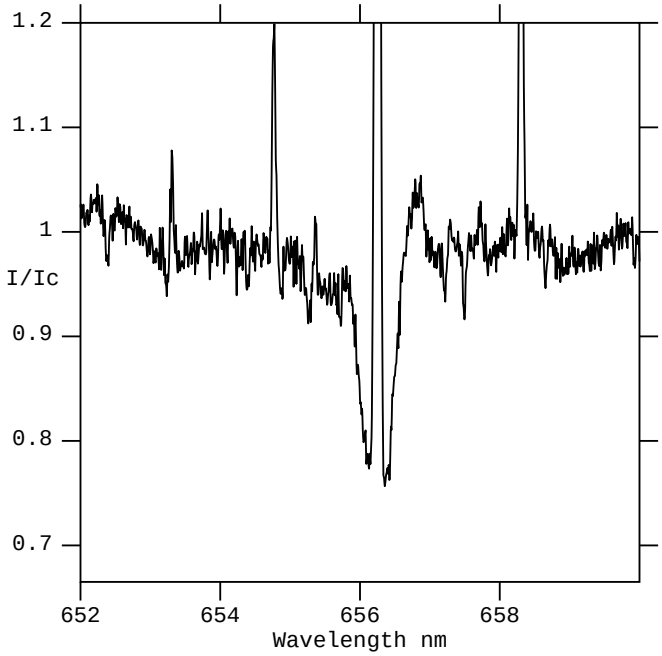

Fig. .12. Same as Fig. .11 but for ELS W080.

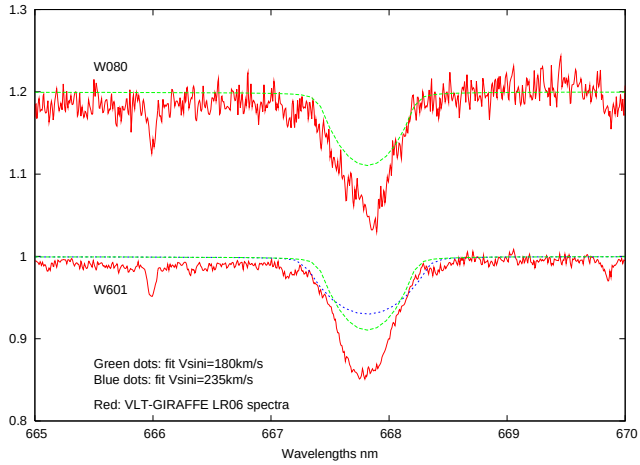

Fig. .13. NLTE model fitting of the HeI 6678 Å from LR06 spectra for the stars W080 (top) and for W601 (bottom). The fundamental parameters used for the fits are those determined for the stars; for W601, 2 different $V \sin i$ were used in function of the studies (Dufton et al. (2006) or Alecian et al. (2008)).

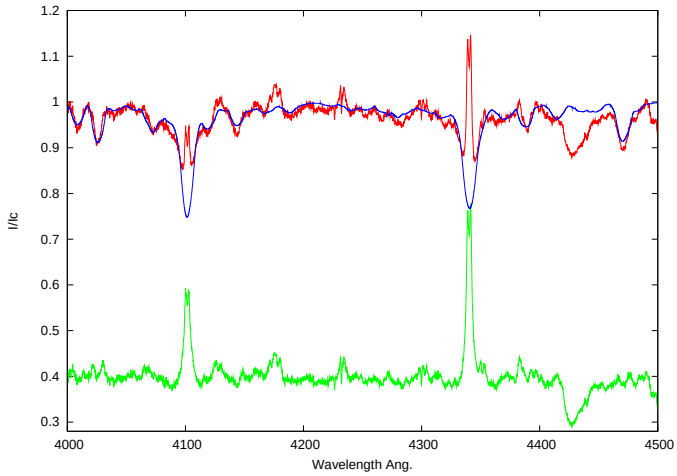

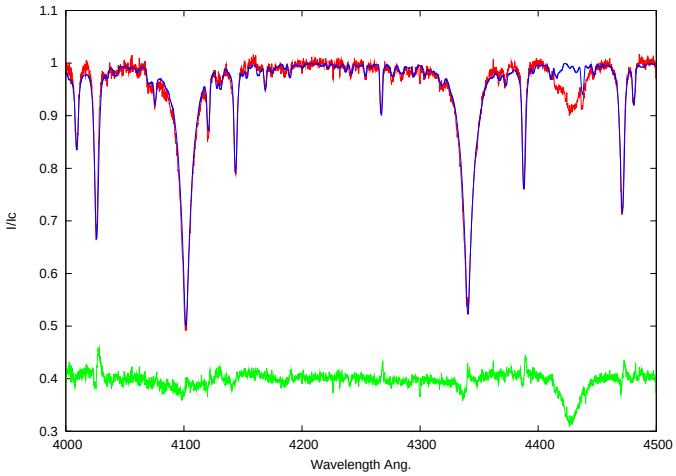

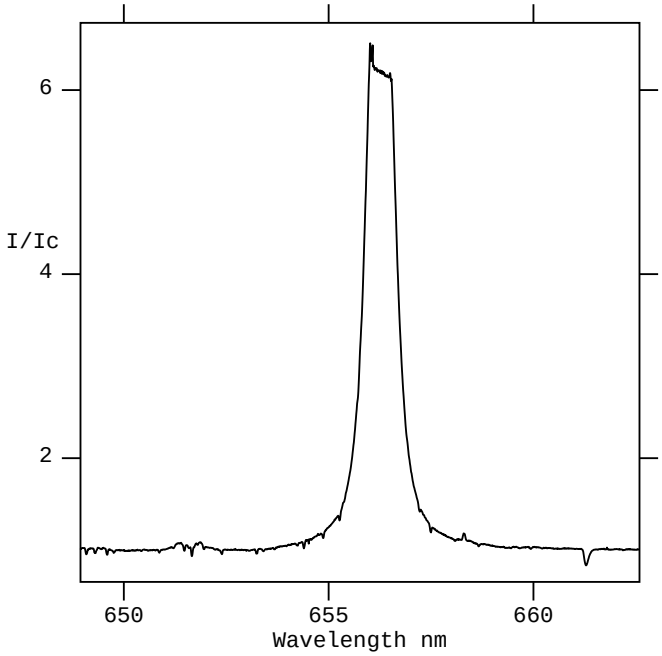

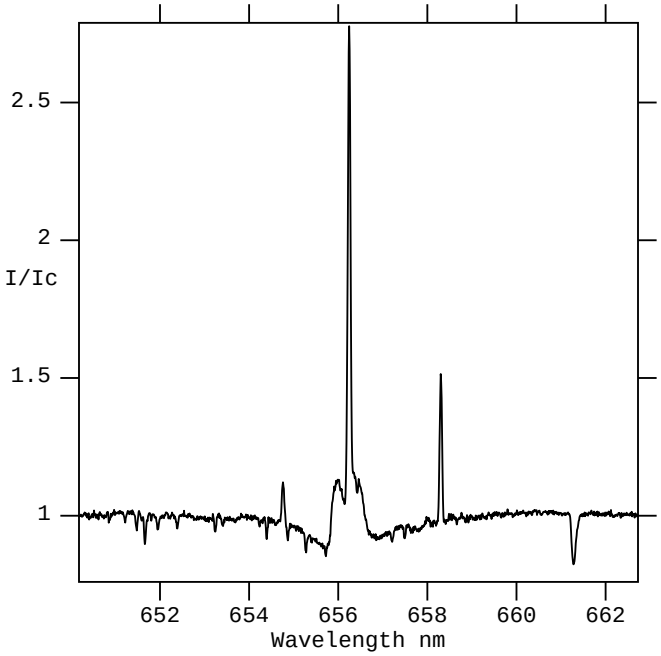

Fig. .15. Same as Fig. .11 but for ELS W301.

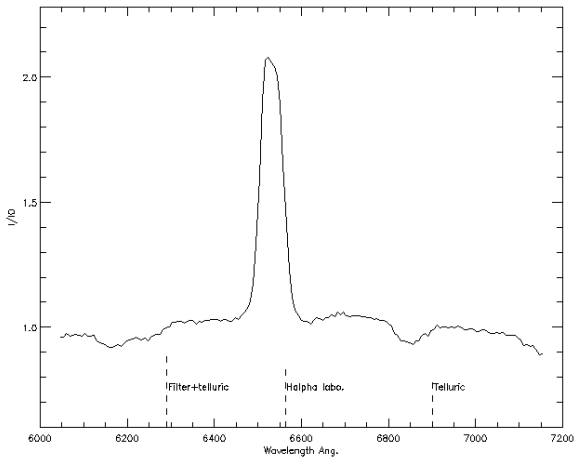

Fig. .14. Same as Fig. .10 but for ELS W235.

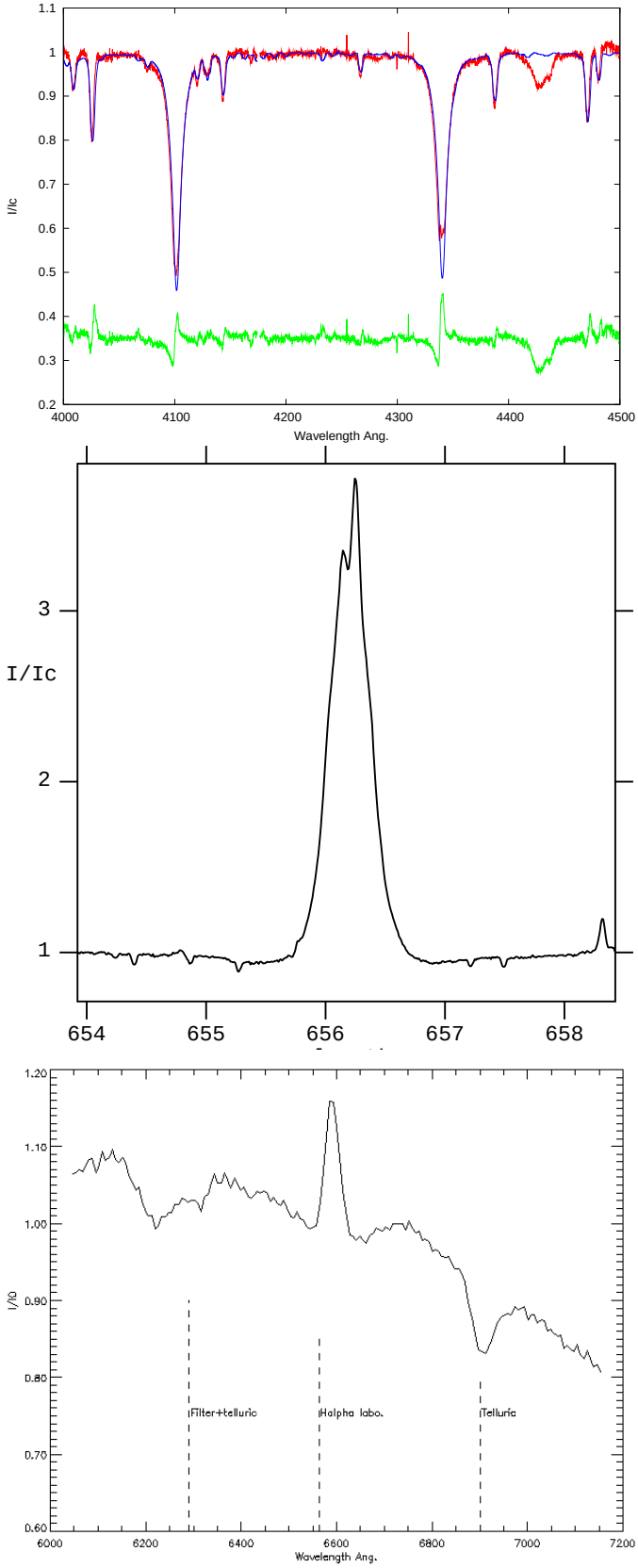

Fig. .16. Same as Fig. .10 but for ELS W483.

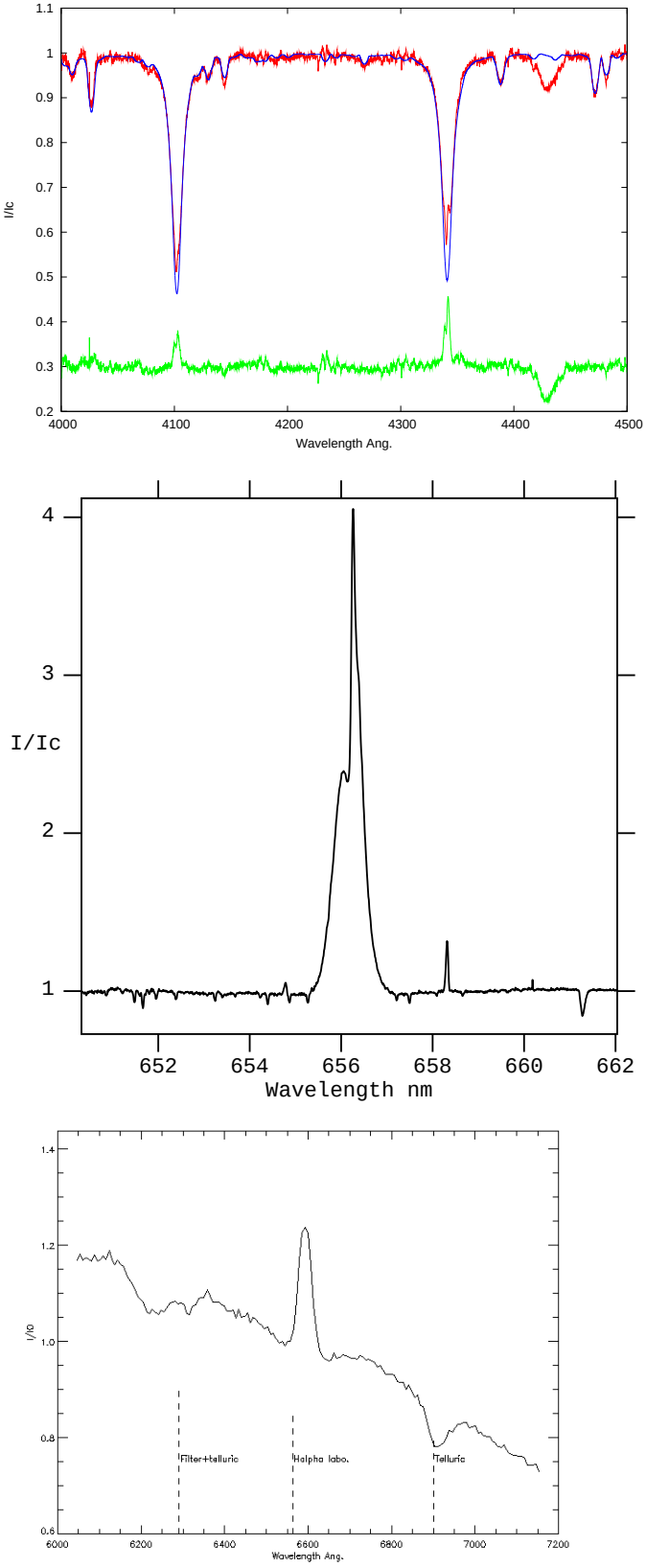

Fig. .17. Same as Fig. .10 but for ELS W500.

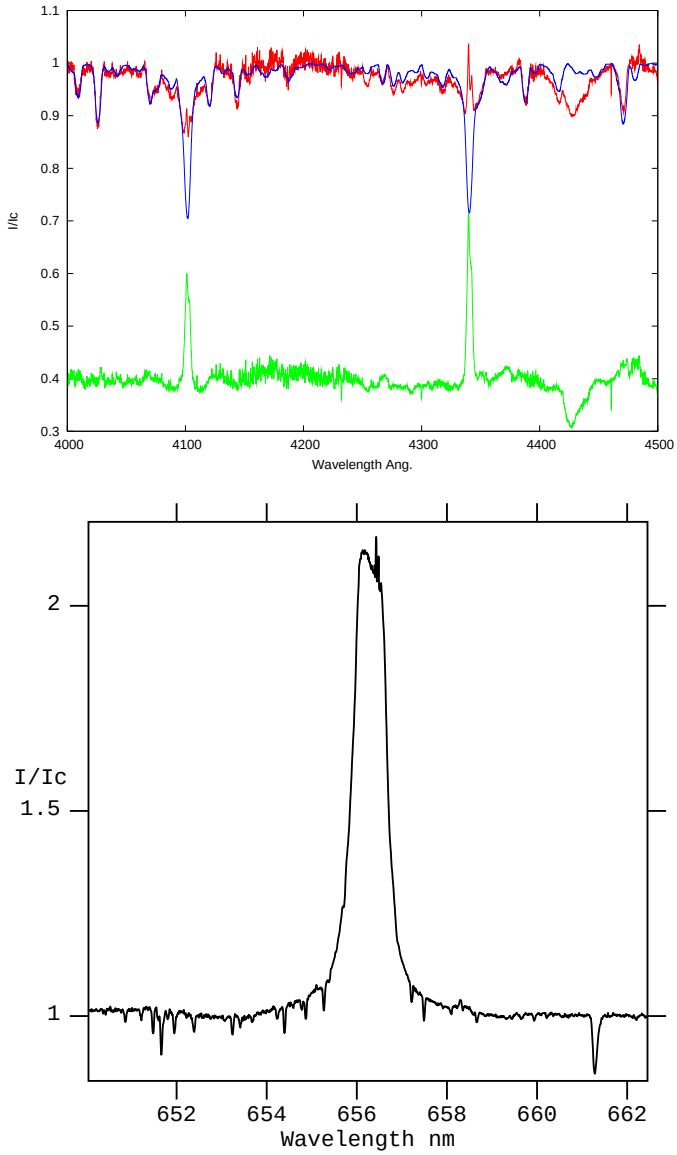

Fig. .18. Same as Fig. .11 but for ELS W503.

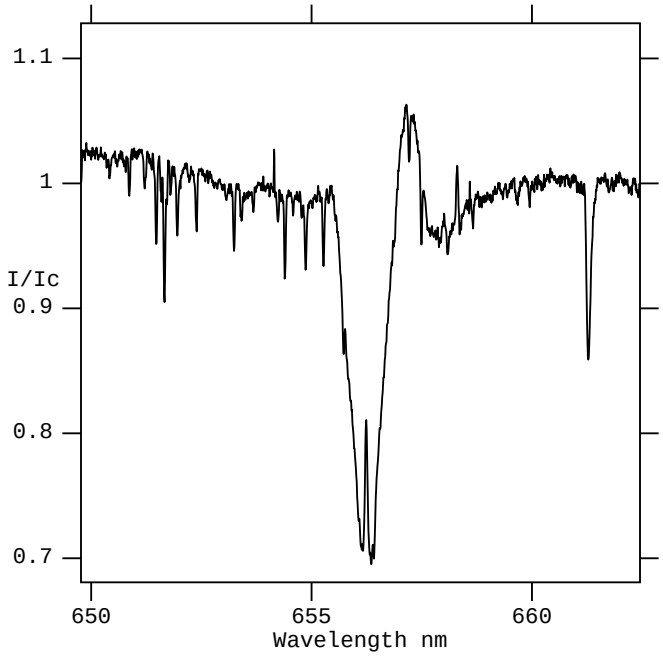

Fig. .19. ELS W601, Hα line from the VLT-GIRAFFE.

List of Objects